Draft version March 20, 2024
Typeset using LaTeX twocolumn style in AASTeX631

The Plane Quasar Survey: First Data Release

Jessica Werk ,[1,2] Kirill Tchernyshyov ,[1] Hannah Bish ,[3] Yong Zheng ,[4] Mary Putman ,[5]
Joshua Peek ,[3] and David Schiminovich [5]

[1]Department of Astronomy, University of Washington, Seattle, WA 98195, USA
[2]Astronomy and Astrophysics Department, University of California, San Diego, CA, 92093, USA
[3]Space Telescope Science Institute, 3700 San Martin Drive, Baltimore, MD 21218, USA
[4]Department of Physics, Applied Physics and Astronomy, Rensselaer Polytechnic Institute, Troy, NY 12180, USA
[5]Department of Astronomy, Columbia University, New York, NY 10027, USA

ABSTRACT

We present a sample of 305 QSO candidates having $|b| < 30°$, the majority with GALEX magnitudes $NUV < 18.75$. To generate this sample, we apply UV-IR color selection criteria to photometric data from the Ultraviolet GAlactic Plane Survey (UVGAPS) as part of GALEX-CAUSE, the Million Quasars Catalog, Gaia DR2, and Pan-STARRS DR1. 165 of these 305 candidate UV-bright AGN (54%) have published spectroscopic redshifts from 45 different surveys, confirming them as AGN. We further obtained low-dispersion, optical, longslit spectra with the APO 3.5-m, MDM 2.4-m, and MDM 1.3-m telescopes for 84 of the candidates, and confirm 86% (N = 72) as AGN, generally with $z < 0.6$. These sources fill a gap in the Galactic latitude coverage of the available samples of known UV-bright QSO background probes. Along with a description of the confirmed QSO properties, we provide the fully-reduced, flux and wavelength-calibrated spectra of 84 low-latitude QSOs through the Mikulski Archive for Space Telescopes. Future HST/COS spectroscopy of these low-Galactic-latitude QSOs has the potential to transform our view of the Milky Way and Local Group circumgalactic medium.

Keywords: Active Galaxies (17) — Quasars (1319) — Circumgalactic medium (1879) — Quasar absorption line spectroscopy(1317) — Milky Way Galaxy (1054) —Ultraviolet astronomy(1736) – Galaxy Spectroscopy (2171)

1. INTRODUCTION

With the recent public data releases from the *Gaia* mission, we now have constraints on positions and velocities for nearly one billion of the Milky Way's stars. This spatial and velocity information from Gaia is especially powerful in combination with benchmark, ground-based surveys such as RAVE (Steinmetz et al. 2006), GALAH (Buder et al. 2018), APOGEE-2 (Majewski et al. 2017), and soon, LSST (Ivezić et al. 2019). Along with data from all-sky surveys covering different wavebands – e.g. HI4PI (HI4PI Collaboration et al. 2016), WHAM (Haffner et al. 2003), Planck (Planck Collaboration et al. 2020), and WISE (Wright et al. 2010) – it is now possible to map three-dimensional stellar age distributions, space motions, and metallicities along with three-dimensional distributions of dust, multiphase gas, and magnetic fields.

Despite impressive progress in building the large datasets necessary for a comprehensive understanding of the Milky Way's evolution, knowledge of the content of our Milky Way's circumgalactic medium (MWCGM) beyond ∼15 kpc remains limited. The MWCGM contains the byproducts of billions of years of star formation, drives its ongoing evolution, and harbors its fuel for future star formation. Unfortunately, it is also one of the most difficult Galactic components to study because we are embedded in a much denser ISM that effectively obscures our view, and because observations of our primary probes of its content, UV-bright background QSOs and halo stars, are biased toward high Galactic latitudes (e.g. Zheng et al. 2015; Bish et al. 2021).

The inner-CGM ($d \lesssim 15$ kpc) of the Milky Way at Galactic latitudes $|b| \gtrsim 30°$ is well-studied. HI 21-cm emission maps of our own Galaxy's halo reveal giant arches, shells, and complexes of neutral clouds moving with $35 < |v_{\rm LSR}| < 250$ km/s, many with distance constraints that place them within the inner halo (Putman et al. 2012). At distances $\lesssim 15$ kpc, ionized diffuse high-velocity gas is distributed over large spatial scales, with a covering fraction of 67%. This gas provides enough potential material to sustain the current level of star-formation in the Milky Way for at least another Gyr (Lehner & Howk 2011; Werk et al. 2019). The velocities and surface densities of this material are generally thought to be consistent with gas cycling in a Galactic fountain, in which hot, over-pressurized gas flows from the disk into the halo, and subsequently cools, recombines and rains back down onto the disk (e.g. Shapiro & Field 1976; Fraternali & Binney 2008). Additionally, there is strong evidence for a more localized, high-energy biconical wind emanating directly from the Galactic Center, observed in emission in hard and soft X-rays, in absorption at UV wavelengths, in polarized radio emission, and in γ rays, referred to as the Fermi Bubble (Snowden et al. 1997; Su et al. 2010; Carretti et al. 2013; Bordoloi et al. 2017; Ashley et al. 2022).

Beyond this very active disk-halo interface region, there is likely a CGM that extends beyond Galaxy's virial radius, similar to other L* galaxies (e.g. Prochaska et al. 2011; Zheng et al. 2019; Wilde et al. 2021, 2023), which contains at least as much mass as in the stars and ISM in the disk itself (e.g. Tumlinson et al. 2011; Werk et al. 2014). Apart from the massive Magellanic Stream (D'Onghia & Fox 2016), we have yet to definitively detect this more extended component, although not for lack of trying. At Galactic latitudes $|b| > 25°$, a QSO-star differencing technique reported significantly less CIV in the CGM of the MW compared to its low-redshift L* counterparts (Bish et al. 2021). This sensitive measurement consisted of subtracting unsaturated absorption lines of the CIV $\lambda\lambda$1548, 1549 doublet toward halo stars with known distances, well above the disk, from the same measurements toward distant QSOs nearby in projection to the stars ($< 2°$). The spectral differencing technique, despite being sensitive to low column densities at v $\sim$ 0, finds mostly *upper limits* on the ionized content of the $>$ 10 kpc MWCGM. However, because all of the Quastar Survey's lines of sight lie at $|b| > 25°$, one option remains to resolve this potential Milky Way anomaly: a very extended, ionized gas disk as has been proposed by Bregman et al. (2018), only visible at low Galactic latitudes.

A major limitation in studies of the Milky Way CGM is a dramatic shortage of UV-bright QSO sightlines at Galactic latitudes $|b| < 25°$, *representing a huge gap that covers approximately half of the sky.* Of the more than 1000 known UV-bright QSOs, only about $\sim$5% of them have Galactic latitudes $|b| < 25°$, and there is only one previously-detected UV-bright QSO confirmed at $|b| < 10°$ (Monroe et al. 2016). Similarly, of the hundreds of QSO lines-of-sight with high-resolution, high-quality *HST*/COS spectra available in the archives, there are only 8 with $|b| < 25°$. UV-bright QSOs near the plane of the Milky Way are notoriously difficult to find because of obscuration by dust and neutral gas, and the lack of deep UV surveys in this area until very recently.

Low-$|b|$ QSOs are critical probes of the structure and kinematics of any extended disk feature that may contribute to the content of the MWCGM. Our Plane Quasar Survey (PQS) addresses this major limitation in our absorption-line studies of the Milky Way by providing a sample of 305 low-Galactic-latitude, UV-bright QSO candidates. In this paper, we confirm $> 60\%$ of these candidates as AGN and provide redshift estimates. Section 2 presents our two selection techniques to identify these low Galactic latitude, UV-bright QSO candidates; Section 3 details the spectroscopic observations for redshift confirmation; and Section 4 provides details on our two methods of deriving redshifts for confirmed QSOs. All of our spectra and tables are available via MAST as a High Level Science Products via https://doi.org/10.17909/86my-mr86[1].

2. CANDIDATE QSO PHOTOMETRIC SELECTION

We use two primary selection techniques to identify low-Galactic-latitude UV-bright QSO candidates. The first uses *NUV* data from the Ultraviolet GAlactic Plane Survey (UVGAPS; Mohammed et al. 2019), which produced a high resolution map of the Milky Way's Galactic plane in the *NUV* using the Galaxy Evolution Explorer (Martin et al. 2005). UVGAPS covers an area of $\sim$ 7200 square degrees (360 degrees $\times$ 20 degrees) with a full width half max resolution of 4.5-6$''$, with 2$''$ pixels, which is a larger footprint at a higher resolution than previous UV all-sky surveys within the same region. We cross-matched the *NUV* source catalog of UVGAPS with the candidate QSOs presented in the Million Quasars Catalog (MilliQUAS; Flesch et al. 2023) to identify candidate UV-bright QSOs, all having $|b| < 10°$ and $NUV < 20.0$. The objects in the MilliQUAS catalog have been selected as likely QSOs using mid-IR color-color classifications from WISE all-sky survey data. Finally, we use *Gaia* parallax data for all targets to exclude those that are likely Galactic stars by imposing a parallax cut of $<$ 0.5 milliarcseconds. In total, this selection method yields 83 Galactic plane quasar candidates.

We supplemented this very low Galactic latitude sample by imposing WISE photometric selection criteria on a broader range of targets from GALEX, similar to the approach of the UVQS Survey (Monroe et al. 2016). Our

[1] https://archive.stsci.edu/hlsp/pqs/

candidate sample selection differs from that of UVQS in that we do not use the *FUV* criteria. Doing so would bias us against targets in the plane of the Milky Way (which UVQS does by design) as the plane was primarily surveyed with GALEX CAUSE when GALEX *NUV* was the only detector available. For this supplementary sample, we select targets from the AllWISE catalog (Cutri et al. 2021) to have $SN > 5$ in $W1$ and $W1-W2 > 0.6$, reject nearby stars by imposing a cut on *Gaia* parallax that requires candidates to have $p < 0.5$ milliarcseconds, and finally select targets with GALEX $NUV < 18.75$ (see 1). We then examined the distribution of $NUV - W2$ colors of the overlapping UVQS-spectroscopically-confirmed QSOs, and imposed an additional color cut of $NUV - W2 > 5$ after discerning that 96% of that sample had $NUV - W2$ colors redder than that limit. Finally, we very conservatively require that our candidates do not exhibit > 6 magnitudes of extinction in the *NUV* (Schlegel et al. 1998). Our final selection criteria for this secondary Plane QSO sample is that $|b| < 30°$. This selection method yielded 222 total QSO candidates. In addition, we note that this supplementary candidate selection does identify 73 (of the 222) QSO candidates that have been previously confirmed as AGN by UVQS.

The coordinates and photometric properties of our complete sample of 305 Plane QSO candidates are provided in Table 1. 165 of these PQS candidates are spectroscopically confirmed as AGN from 45 different spectroscopic surveys, and the quoted spectroscopic redshifts and references, when available, are also provided in Table 1. Because the data come from a variety of surveys, with varying spectral properties and redshift accuracy, we refer readers to the original source papers for details. Generally, the lowest Galactic latitude PQS candidates from the UVGAPS selection method are the ones without archival redshifts, and we prioritized these for our own spectroscopic followup, described in subsequent sections. However (somewhat accidentally), we re-observed 45 of these sources with existing spectroscopic data. In part, this was due to not completing a full archival cross-matching of our candidates before commencing our observing runs. These re-observed targets allow us to compare QSO redshifts derived from different telescopes and instruments, which we discuss in Section 4.

In Figure 1, we show a color-magnitude plot of *WISE* and *GALEX* photometry for the 1055 confirmed AGN in UVQS and for the 305 Plane QSO candidates whose selection is described above. Our set of UVQS-like photometric selection criteria are shown as dashed lines. The *WISE* magnitudes are drawn from the all-WISE Source catalog ("w2mpro" and "w1mpro"), and

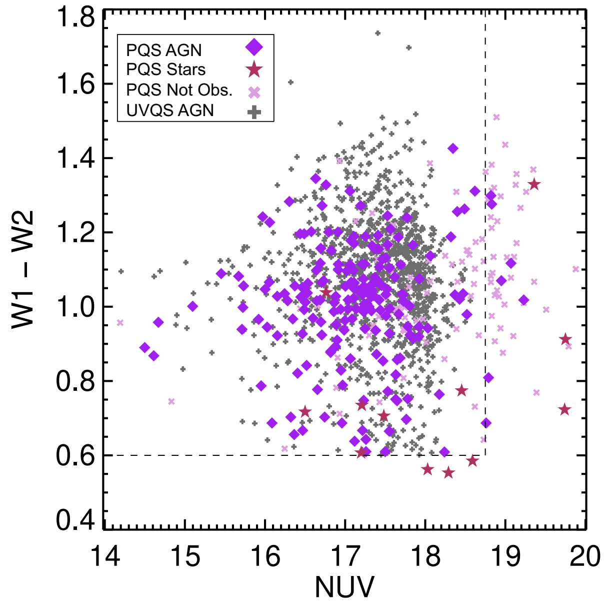

Figure 1. UV-bright QSO Photometric Selection: A WISE-GALEX color-magnitude diagram showing the distribution of different UV-bright QSO samples in GALEX NUV magnitude vs $W1-W2$ color, including the our Plane QSO candidates from both selection methods (dark and light purple shapes). The gray plus signs show the confirmed AGN from the UVQS Survey (Monroe et al. 2016), including those that were previously identified by the Milliquas Survey (Flesch 2023). Purple diamonds highlight the spectroscopically-confirmed low-latitude QSOs, which fill a gap in the existing datasets. The 12 maroon stars show objects in our candidate list that are spectroscopically confirmed as stellar sources, and the light purple x's are targets from our candidate list that have not yet been observed.

are measured from profile-fitting photometry, while the *GALEX NUV* magnitudes are drawn from the band-merged source catalog GR6 data on MAST. The distribution of both samples within this $WISE - GALEX$ color magnitude diagram overlaps considerably. Every candidate and confirmed source that lies outside of these bounds originates in the first candidate selection method that uses UVGAPS data and the MilliQUAS catalog. Overall this sample does not appear markedly different from the sample selected from the second-set of criteria described above. The dark purple diamonds in Figure 1 show our Galactic plane QSO candidates that are spectroscopically confirmed as AGN, while the dark maroon stars show candidates that exhibit stellar spectra. Light purple x's show Plane QSO candidates that remain unobserved.

Figure 2 shows the all-sky distribution in Galactic coordinates of our sample of candidates, as well as the UVQS confirmed AGN and AGN with high-SN

UV spectroscopy in the *Hubble Spectroscopic Legacy Archive* (Peeples et al. 2017). Compared to previously-catalogued UV-bright AGN, our Plane QSO candidates, by design, generally lie at lower Galactic latitudes and are most numerous at Galactic longitudes $l > 90°$. The dark purple diamonds and stars in Figure 2 show the 84 objects for which we have obtained spectra and those objects with archival spectroscopic redshifts available. Our initial data release for the Plane QSO survey represents a spectroscopic completeness of ∼63%. Given the finite lifetime of *HST*/*COS*, we believe the public release of this limited dataset to be both important and timely, especially given that many of the targets lie in areas of interest completely devoid of existing high-resolution UV spectroscopy.

3. OBSERVATIONS AND DATA PROCESSING

In total, we obtained spectra of 84 Plane QSO candidates during the 2020 calendar year. For the majority of the candidates we observed, we obtained low-dispersion, longslit optical spectra using the APO 3.5-m telescope with the *DIS* spectrograph and with the MDM 2.4-m telescope with the OSMOS spectrograph. For six candidates, we obtained spectra on the MDM 1.3-m telescope using CCDS. We generally prioritized targets with the lowest latitudes and brightest UV magnitudes such that they would be ideal sources for *HST*/COS follow-up to kinematically isolate any extended, ionized features in the Galactic plane. In addition, we prioritized potential lines of sight at Galactic longitudes that are optimal for isolating extended structures in a rotating disk, observed 8 kpc from its center. Specifically, we looked primarily at Galactic longitudes that are looking away from Galactic center ($l = 0°$) and anti-center ($l = 180°$), and either toward or against the direction of rotation, respectively $l \approx 90°$, and $l \approx 270°$. This section details the observations on each telescope, and describes the properties of the reduced, one-dimensional, calibrated spectra.

All of our calibrated, 1D spectra are available at MAST as a High Level Science Product via https://doi.org/10.17909/86my-mr86[2]. Given the range of instruments employed, and the diversity of targets, the resultant spectra are of varying quality. The S/N ranges from 3 − 100. We note that every target we observed has a spectrum of sufficient quality to determine a source type (e.g. star or AGN), as well as a redshift if the target was an AGN.

3.1. *Optical Spectroscopy with the APO 3.5-m*

3.1.1. *Description of Observations*

APO data were taken under largely clear skies with variable atmospheric conditions over the course of four grey-time half-nights in February, October, and December of 2020. We used the *Dual Imaging Spectrograph* (DIS), which has a spatial scale of ∼0.4″/pixel, with the R300 grating in the red channel. All spectra were taken with a 1.2″ slit, which was the approximate seeing on each night we were able to observe. Our APO red-channel instrumental setup results in a linear dispersion of 2.31Å/pixel and a spectral coverage of 4620Å about a central wavelength of 7500Å. During our runs, the blue channel of DIS was not functional so we were only able to use the red channel. Each candidate was observed with a 600-second exposure time.

3.1.2. *Data Reduction and Final Products*

The APO two-dimensional spectra were reduced and calibrated using a custom python package *pydis*[3] developed by J. Davenport. The spectra are bias-subtracted, flat-fielded using quartz lamp images in the same spectral configuration as the data, and wavelength-calibrated using Hg-Ne-Ar arc-lamp exposures. The wavelengths were then shifted to a vacuum and heliocentric reference frame. The wavelength solutions have a typical rms of 0.8 Å. The targets were extracted to one-dimensional spectra using an optimized aperture, and were flux-calibrated in a relative sense using observations of a spectrophotometric standard star taken during twilight each night. The flux calibration is coarse – we have not corrected for slit-losses and only observed the standard star during twilight on nights during which the conditions were highly variable. Nonetheless, the calibration that is applied should allow for an approximate comparison of emission-line fluxes in QSO spectra in a relative sense. The average S/N of each spectrum is 18 per resolution element, and each spectrum is high-enough quality to allow us to determine the source-type, and redshift if it is extragalactic.

3.2. *Optical Spectroscopy with the MDM 2.4-m and 1.3-m*

3.2.1. *Description of Observations*

MDM 2.4-m spectra were obtained with the Ohio State Multi-Object Spectrograph (OSMOS) in queue-mode observing from November - December 2020. OSMOS has a spatial scale of ∼0.3″/pixel. Every target was observed for 600s with the MDM4K detector, a 1.2″ slit, and the VPH blue grism with $R = 1600$ (dis-

[2] https://archive.stsci.edu/hlsp/pqs/

[3] https://github.com/StellarCartography/pydis

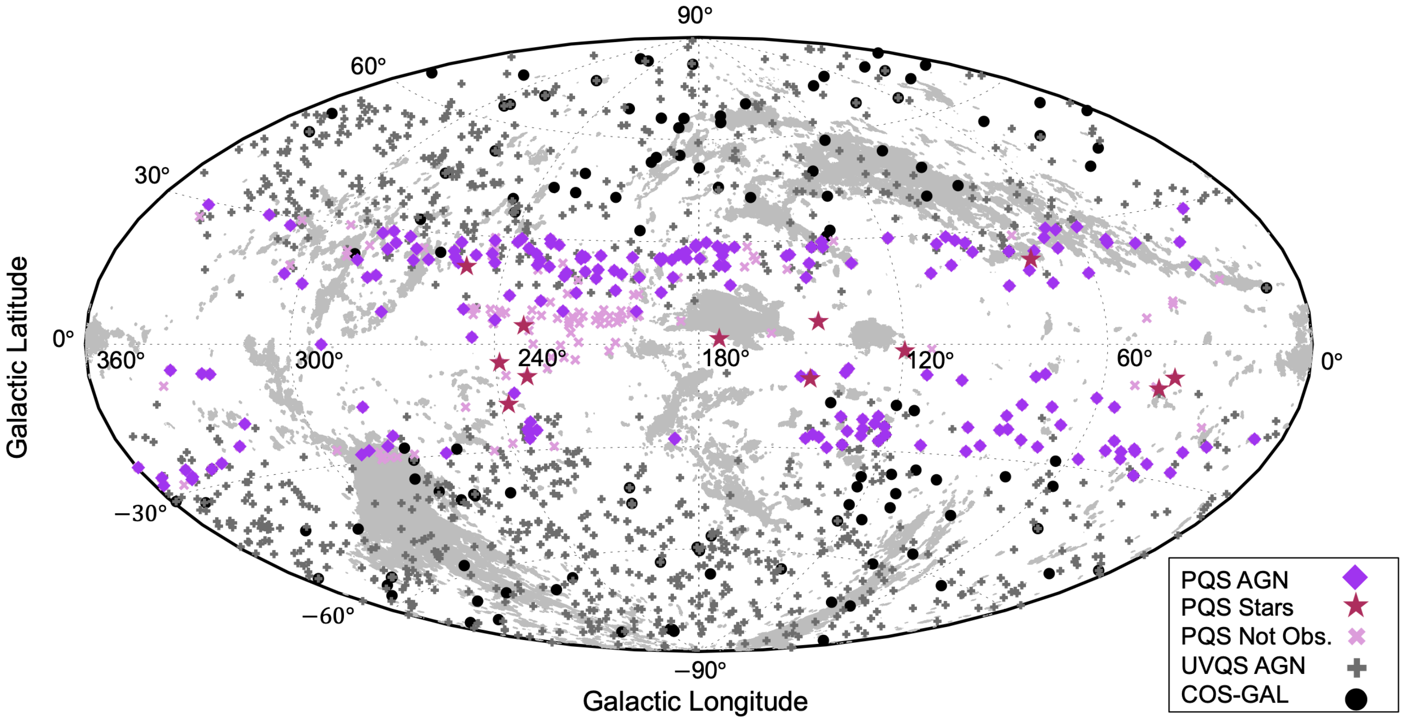

Figure 2. UV-bright QSO All-Sky Distribution: An all-sky Aitoff projection in Galactic coordinates, centered at $b = 0°$, $l = 180°$, showing the distribution of different UV-bright QSO samples, including the Plane QSO candidates (dark and light purple shapes). For orientation within this frame of reference, the underlying gray map shows high-velocity ($|v_{\rm LSR}| > 80$ km s^{-1}) HI detected in 21-cm emission from the HI4PI Survey (HI4PI Collaboration et al. 2016; Westmeier 2018), generally with $N_{\rm HI} > 10^{18}$ cm^{-2}. The black circles show the 401 archival QSO sightlines with high-resolution *HST*/COS spectra from the COS-GAL database (Zheng et al. 2019) , and the gray plusses show all the confirmed AGN from the UVQS Survey (Monroe et al. 2016), including those that were previously identified by the Milliquas Survey (Flesch 2023). Purple diamonds highlight the spectroscopically-confirmed low-latitude QSOs, which fill a gap in the existing datasets. The 12 stars show objects in our candidate list that were confirmed stellar sources, and the light purple x's are targets from our candidate list that have not yet been observed.

persion ≈ 0.7Å/pixel). The grism uses an inner and center slit with wavelength coverages of 3900 − 6800 Å (inner) and 3100 − 5950 Å(center). Three of our targets were observed remotely on the 1.3-m with the Boller and Chivens CCD Spectrograph (CCDS) in February and March of 2020 under moderately unfavorable atmospheric conditions. On the 1.3-m, CCDS has a spatial scale of ∼0.4″/pixel. For these targets, we exposed for 600s using a 1.5″ slit, and used the 150 l/mm grating with a central wavelength value of 5500 Å, which has a dispersion of ∼3.3Å/pixel.

3.2.2. *Data Reduction and Final Products*

MDM spectra were reduced using the IRAF *specred* package (Tody 1993; Valdes 1992), which includes bias subtraction, flat-field calibrations using quartz lamp images, and wavelength calibration using Hg-Ne-Ar arc-lamp exposures. We shifted all wavelengths to a vacuum and heliocentric reference frame. The wavelength solutions for the OSMOS data have a typical rms of 0.4 Å, whereas those of CCDS are 1.4 Å. We performed the extraction of the 1D spectrum using the *APALL* task, and manually adjusted each aperture size in an interactive procedure to contain the majority of the target flux. We flux-calibrated the data using observations of several spectrophotometric standard stars, all observed during twilight time, generally to a relative accuracy of ∼10%.

4. REDSHIFT DETERMINATION

The primary goal of this paper is to provide spectroscopic confirmation of low-*b*, UV-bright QSO candidates and to determine an approximate redshift. Visual examination of our 84 reduced QSO candidate spectra revealed that 12 of these candidates are very likely stars, with spectra generally consistent with G and M dwarfs. We list these stars and the telescopes at which their spectra were taken, in Table 2, along with the 72 confirmed AGN sources. The majority of the confirmed stellar sources (8/12) come from our UVGAPS selec-

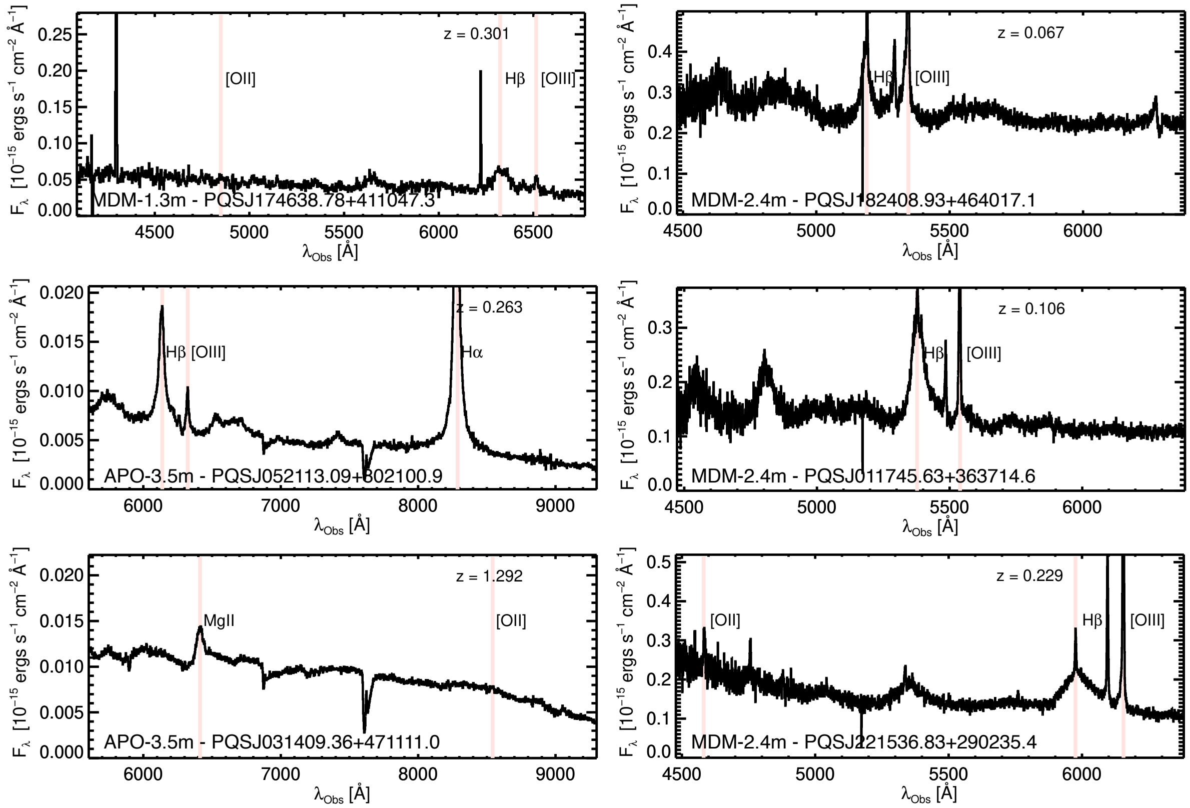

Figure 3. Example PQS Spectra: We show six flux and wavelength-calibrated, 1D spectra from the three different telescopes used during our PQS observing runs. On the upper right of each panel, we provide the MARZ redshift determined using the template QSO spectrum fits. Some of the strong emission lines identified in each spectrum are labeled, and the telescope and PQS target name are given in the lower right hand corner of the spectra. All of the spectra are available to download on MAST.

tion, and tend to lie at $|b| \lesssim 10°$ (11/12). We note that our UVGAPS selection technique yielded a lower AGN-confirmation rate (9/17; 53%) than our UVQS-like sample selection method (63/67; 94%), likely because the former sample is more concentrated along the Galactic plane, where stellar contamination will naturally be higher. We consider the stars no further in our analysis.

Uncertainties in deriving systemic redshifts from broad emission lines in low-dispersion optical spectra of QSOs often exceed 500 km s^{-1}, and individual redshift measurements for the same QSO can differ by up to 1000 km s^{-1}, depending on which lines are used in the fitting algorithm (e.g. Stoughton et al. 2002). By comparison, errors from wavelength calibration alone are $\sim$ 50 km s^{-1} for our low resolution optical spectra. Well-tuned methods of template spectral fitting and spectral masking can reduce QSO redshift errors by a factor of twenty (Hewett & Wild 2010), but again, depend on the specific emission lines that are present in the spectrum. For example, using narrow [OII] and other low-ionization lines for redshift measurements may offer significant advantages over [OIII]-based redshift measurements, which often show signs of outflows and shifts of up to 400 km s^{-1} with respect to stellar absorption lines (e.g. Boroson 2005; Shen et al. 2016). With these caveats and realities in mind, we employ two methods to estimate the redshifts of our confirmed AGN sources with heterogenous spectral quality and wavelength coverage. When possible, we compare our independently-derived redshift measurements with those available in the literature for the same QSOs.

Figure 3 shows six one-dimensional, flux and wavelength calibrated PQS spectra of varying quality, with at least one from each of the telescopes we used for spectroscopic confirmation. Identified emission lines are labeled in each panel, and the redshift of each source is labeled in the upper right corner of each spectrum. Note, the spectra have not been cleaned of cosmic rays and are not corrected for telluric absorption. Because the targets span a range of redshifts, and were observed using different instruments and set-ups, we see a variety of emission lines in each spectrum. Generally, all of our spectra contained at least one feature that allowed us to determine its spectral type and redshift.

In our first redshift estimation, we used MARZ, Manual and Automated Redshifting Software (Hinton et al.

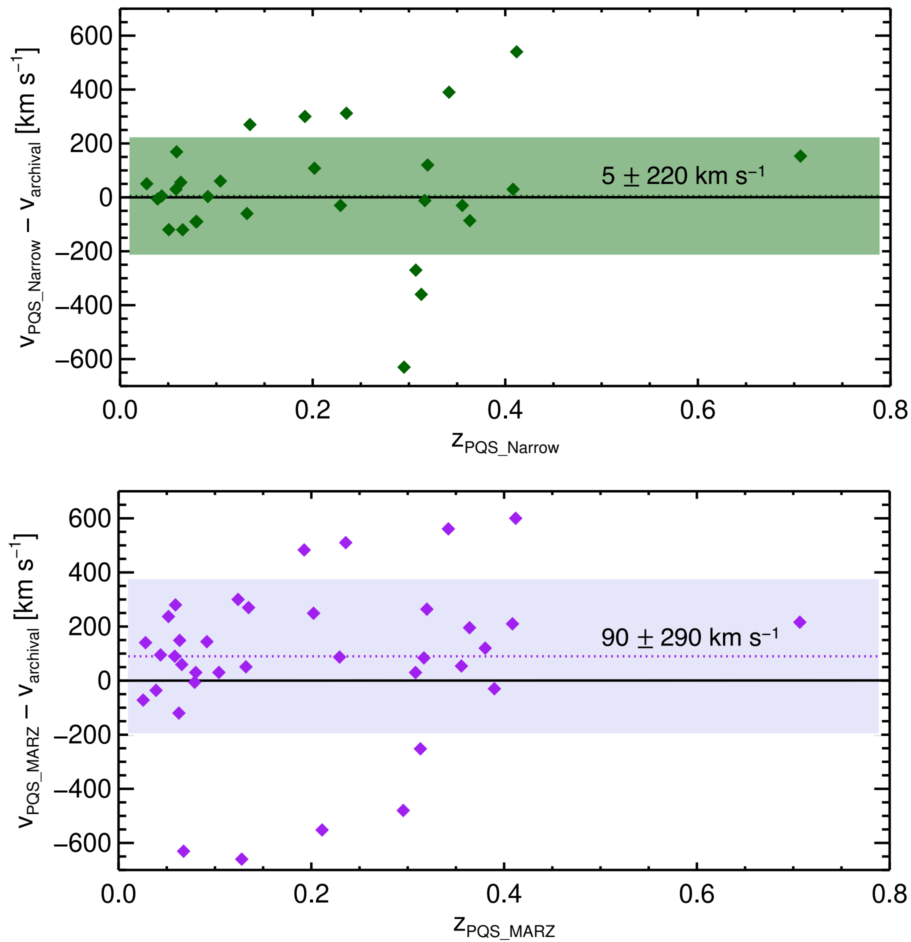

Figure 4. Top: We compare our redshifts derived from narrow-line fits (generally to [OIII] $\lambda\lambda$ 4960, 5008) with those available in the literature, from different sources, determined with a variety of methods based on data of highly variable quality. Bottom: We compare our MARZ template-fitted QSO redshifts with those same literature QSO redshift estimates. On both panels, we have labeled the mean velocity offsets between the PQS redshifts and archival estimates with $\pm$ 1σ spreads. We have eliminated from this analysis the eight cases discussed in the text with $>$ 1000 km s^{-1} differences.

2016). We interactively fit a template QSO spectrum to our 1-D, flux and wavelength-calibrated spectra, and in approximately 30% of the cases, the automatic algorithm finds a high-quality redshift that appears to match the QSO features in the spectra (rather than, e.g., a spurious cosmic ray or a poorly-subtracted sky line). We hypothesize that the automated fitting routine fails in the majority of cases because our PQS spectra are uncleaned for cosmic rays and telluric absorption; both appear to be affecting the MARZ automated algorithm. In the majority of our spectra, we have to manually adjust the redshift to our "by-eye" estimate based mostly on line identifications of the Balmer series lines and [OIII] λ 5008, and then re-run the template fitter. The variance in redshift fitting results reported by Hinton et al. (2016) is generally very low ($\Delta z/(1+z) \approx 3 \times 10^{-4}$). Observational errors (e.g. wavelength calibration) and systematic errors (e.g. ubiquitous QSO outflows) will dwarf these fitting errors. As discussed above, the errors on our redshifts are likely well above 100 km s^{-1}.

Our second redshift estimation is made using Gaussian fits to only the narrow emission lines present in the QSO spectra. For approximately 25% of the sample, only broad Balmer lines or the MgII doublet are detected, and so we cannot employ this secondary redshift estimate. In the majority of cases in which narrow lines are present, we use the [OIII] lines at $\lambda\lambda$ 4960, 5008. The [OII] doublet at $\lambda\lambda$ 3727, 3729 is blended together at these low spectral resolutions, and is often in a very noisy region of the spectrum and thus not often well-detected. Hewett & Wild (2010) find systematic offsets of [OIII]-derived redshifts of 45 $\pm$ 5 km s^{-1} to the blue in comparison to centroids from the CaII K absorption line at 3934.8 Å, however we do not apply this shift to our narrow-line redshift estimates.

We provide both of these redshift estimates, in addition to the archival redshift estimate and its source, in Table 2. We compare our two redshift estimates with those values we find in our archival reference sample in the upper and lower panels of Figure 4. Given the variety of origins of the spectra, we are not implying that the reference redshifts are more or less correct than our values, but instead showing the typical variance in redshift estimates for the same sources. Our narrow-line redshifts agree reasonably with the previously published values, with a mean offset of only 5$\pm$ 220 km s^{-1}. Our MARZ-template-fitting-derived redshifts are biased high by 90 $\pm$ 290 km s^{-1}, but this is not significant considering we expect our QSO redshift errors to be hundreds of km s^{-1}.

Not included in Figure 4 are eight sources with redshift estimates that differ from the published values by more than 1000 km s^{-1}, well outside of our expected errors. We consider these sources highly discrepant. That said, the source of the large errors in the majority of cases is almost certainly rounding error. In 7/8 discrepant cases, the published redshifts are given to only two significant figures, which means differences larger than 1000 km s^{-1} are expected. The remaining true discrepancy is PQSJ211452.57+060742.9, or 2MASS J21145258+0607423. The published redshift value for this QSO is 0.457 (O'Meara et al. 2017), compared to our MARZ redshift of 0.4608, derived from two very broad emission lines we identified as MgII and Hγ. O'Meara et al. (2017) state the wavelength covered in the Keck spectrum to be $3805 - 5976$ Å, and thus, they would have detected only the broad MgII line for a redshift estimate. A redshift uncertainty of $\pm$ 1000 km s^{-1} is therefore appropriate for this target.

5. SUMMARY

In this paper, we have presented 305 low-Galactic-latitude, UV-bright QSO candidates that move us closer to unbiased coverage in Galactic coordinates of UV-bright background probes of the MWCGM. Of the 84 candidates we observed with low-resolution, ground-based spectroscopy from MDM and APO, we confirmed 72 as AGN. Combined with archival redshift estimates, our redshift estimates for these 72/84 (86%) confirmed AGN bring us to 193 / 305 (63%) spectroscopically-confirmed, UV-bright QSOs at low Galactic latitudes. When possible, we compare our redshifts with those available in the archives via a SIMBAD crossmatch and generally find good agreement to within $\pm$ 200$-$300 km s^{-1}. We make our full catalog, redshift estimates, and spectra publicly available via MAST as a High Level Science Product via https://doi.org/10.17909/86my-mr86[4] in hopes that it will be used in future studies of the Milky Way and Local Group CGM while HST/COS is still available.

6. ACKNOWLEDGEMENTS

We thank the dedicated telescope support staff at both APO and MDM observatories, especially for making these remote observations possible during a global pandemic. In addition, J.K.W. would like to thank the newly formed Department of Astronomy and Astrophysics at UC San Diego, especially Alison Coil and Dusan Keres, for welcoming her to their beautiful campus as a Margaret Burbidge Visiting Professor during Winter 2024. J.K.W. is also deeply thankful for Laura Chomiuk and Kate Rubin, whose regular support through mutual accountability makes it possible to complete projects like this one while also juggling the responsibilities of being faculty. This research has made use of the SIMBAD database, operated at CDS, Strasbourg, France (Wenger et al. 2000), and the HSLA database, developed and maintained at STScI, Baltimore, USA. Support for this work was provided by NSF-CAREER 2044303.

Facilities: McGraw-Hill, Hiltner, ARC

Table 1. Plane QSO Candidates

PQS Name	SIMBAD Name	l	b	m_{NUV}	W1−W2	Ref z	Ref
PQSJ002324.76+605103.6	IRAS 00206+6034	119.5240	-1.8350	16.50	0.72		
PQSJ004342.52+372520.1	LEDA 2100384	121.2328	-25.4239	16.74	0.70	0.0800	2015RAA....15.1438H
PQSJ004818.93+394112.1	2MASS J00481898+3941116	122.2785	-23.1810	16.71	0.92	0.1340	2016ApJ...818..113N

Table 1 *continued*

[4] https://archive.stsci.edu/hlsp/pqs/

Table 1 *(continued)*

PQS Name	SIMBAD Name	l	b	m_{NUV}	W1−W2	Ref z	Ref
PQSJ005050.78+353644.0	2MASS J00505073+3536429	122.7967	-27.2593	16.47	0.93	0.0580	2016AJ....152...25M
PQSJ010131.18+422935.1	2MASS J01013117+4229356	124.9137	-20.3397	16.94	0.99	0.1900	2016ApJ...818..113N
PQSJ010415.84+402243.5	UVQS J010415.77+402243.9	125.5740	-22.4271	16.50	1.01	0.1910	2016AJ....152...25M
PQSJ011745.63+363714.6	2MASS J01174562+3637144	128.8032	-25.9506	17.51	1.03	0.1100	2015RAA....15.1438H
PQSJ011849.46+383618.8	[VV2000] J011849.5+383619	128.7829	-23.9551	17.92	0.92	0.2200	2015RAA....15.1438H
PQSJ012400.58+410709.9		129.5100	-21.3358	17.57	1.21		
PQSJ013741.29+330934.9	3C 48	133.9625	-28.7194	17.33	1.06	0.3690	2016AJ....152...25M
PQSJ013925.09+370454.9	LEDA 2092626	133.4563	-24.8072	17.39	0.87		
PQSJ015536.05+311518.3	LEDA 3095555	138.7027	-29.6440	17.63	0.82	0.1334	2020ApJS..250....8L
PQSJ015756.87+402413.3	UVQS J015756.83+402413.1	136.4040	-20.7216	16.70	1.16	0.4580	2016AJ....152...25M
PQSJ021248.58+330643.3	ATO J033.2024+33.1119	141.9604	-26.7352	17.69	1.11		
PQSJ021935.13+534019.9		135.8717	-6.9702	17.26	0.61		
PQSJ022206.31+522106.1	2MASS J02220630+5221059	136.6858	-8.0820	18.37	1.03	0.2000	1991A&A...246L..24M
PQSJ022232.00+330622.1	QSO B0219+3252	144.0787	-25.9975	17.41	1.19	0.5040	1993AJ....105..660W
PQSJ022814.48+311841.3	NGC 931	146.1141	-27.1659	16.69	1.12	0.0168	2018ApJ...861...49H
PQSJ031304.24+461120.7		146.9644	-9.9689	19.75	0.91		
PQSJ031409.36+471111.0		146.5947	-9.0222	18.82	1.30		
PQSJ032839.48+451440.5	2MASS J03283948+4514404	149.7976	-9.2689	20.14	1.05		
PQSJ040821.86+604649.4	ATO J062.0910+60.7803	144.7800	6.5612	19.74	0.72		
PQSJ042630.15+070530.4	[VV2000] J042630.1+070530	187.6921	-27.7578	17.42	1.16	0.1700	1999A&AS..134..483H
PQSJ042704.25+071632.5	[OKM2018] SWIFT J0427.0+0734	187.6167	-27.5359	17.37	1.16	0.0960	1990AJ....100.1274W
PQSJ045640.88+482058.0	ATO J074.1703+48.3493	158.6602	3.2549	16.93	0.71		
PQSJ052113.09+802100.9	2MASS J05211320+8021011	132.6207	23.0984	17.23	1.07		
PQSJ052409.90-235455.6		226.5674	-29.1585	17.97	0.97		
PQSJ053715.36+345344.8	Gaia DR2 3449698082675788928	174.0027	1.6442	18.29	0.55		
PQSJ054323.09-285841.2	2MASS J05432311-2858410	233.5341	-26.6613	17.81	0.92	0.2286	2009MNRAS.399..683J
PQSJ054324.55-403046.8		246.1879	-29.6119	18.62	1.10		
PQSJ054508.41-342205.8	USNO-A2.0 0525-02348261	239.4666	-27.8375	18.71	1.18		
PQSJ054917.25-254810.0	2MASS J05491725-2548098	230.6680	-24.4004	17.02	1.10	0.5960	2016AJ....152...25M
PQSJ055002.09-281312.2	2MASS J05500211-2813124	233.2415	-25.0378	17.51	0.98	0.1520	2016AJ....152...25M
PQSJ055425.29-280544.8	UVQS J055425.28-280544.6	233.4567	-24.0828	16.65	0.78	0.0630	2016AJ....152...25M
PQSJ055447.23+662043.4	2MASS J05544724+6620438	147.2725	19.2873	16.05	1.07	0.1870	2016AJ....152...25M
PQSJ055714.69-535714.1	IRAS 05562-5357	261.8740	-29.4305	17.24	1.05	0.0967	2001ApJ...546..744N
PQSJ055925.75-723844.7		283.3914	-29.6666	16.66	1.00		
PQSJ060105.70-261108.9	LEDA 3081156	232.0496	-22.0393	16.47	0.67	0.0390	2009MNRAS.399..683J
PQSJ060323.15-680437.5		278.1284	-29.4833	17.30	0.92		
PQSJ060410.06-700422.6	MGPN LMC 85	280.4192	-29.3934	18.40	1.07		
PQSJ060529.04-625450.3	1RXS J060529.1-625442	272.2162	-29.1229	17.55	1.17		
PQSJ060819.91-715738.1	IRAS 06091-7157	282.5740	-29.0191	15.64	2.04		
PQSJ062204.09-773101.7	6dFGS gJ062204.2-773101	288.8777	-28.0206	16.99	0.94	0.1125	2009MNRAS.399..683J
PQSJ062255.49-720740.8	SMP LMC 100	282.7771	-27.8963	18.06	1.07		
PQSJ062409.79+273957.6	2MASS J06240980+2739574	185.2582	6.7846	19.51	0.99		
PQSJ063002.55+690504.3	QSO B0624+6907	145.7085	23.3485	15.45	1.09	0.3740	2016ApJ...818..113N
PQSJ063117.46-290730.7	ATO J097.8228-29.1251	237.5212	-16.8695	18.45	0.77		
PQSJ063224.57+045937.6	NGC 2244 245	206.3163	-1.9389	18.62	0.73		
PQSJ063301.43+622543.2	2MASS J06330145+6225436	152.7234	21.7860	17.58	1.10		
PQSJ063403.59-744637.8	2MASS J06340353-7446377	285.8061	-27.2379	16.35	0.97	0.1120	2014A&A...561A..67P
PQSJ063626.08-684821.2	[VV2000] J063625.6-684822	279.1595	-26.4995	17.34	1.16	0.3330	2016AJ....152...25M
PQSJ063737.12+074819.4	Gaia DR2 3133893569808649856	204.4153	0.5038	18.73	0.64		
PQSJ064011.77-255342.1	ESO 490-26	235.2352	-13.7918	17.23	0.75	0.0258	2009MNRAS.399..683J
PQSJ064134.44-050234.8	PN We 1-5	216.3069	-4.4866	18.60	0.00		
PQSJ064139.39+451002.0	2MASS J06413937+4510020	170.4583	17.2534	17.11	1.17	0.2970	2016AJ....152...25M
PQSJ064754.31-132823.5	2MASS J06475433-1328235	224.5843	-6.8679	18.94	0.94		
PQSJ064958.63-073852.7	2MASS J06495854-0738522	219.5829	-3.8019	17.43	0.74		

Table 1 *continued*

Table 1 *(continued)*

PQS Name	SIMBAD Name	l	b	m_{NUV}	W1−W2	Ref z	Ref
PQSJ065030.88-195929.0	2MASX J06503094-1959267	230.7776	-9.1639	18.59	0.59	0.0258	2002LEDA.........0P
PQSJ065154.68-405846.8	2MASS J06515469-4058473	250.6734	-17.3160	18.90	1.04		
PQSJ065342.55+165317.8		198.0526	8.1003	18.92	1.03		
PQSJ065435.35+172204.0		197.7097	8.4991	19.07	1.08		
PQSJ065629.87-653337.1	FRL 265	276.0061	-24.0163	15.95	0.79	0.0305	2011MNRAS.416.2840L
PQSJ065711.42-105729.1	2MASS J06571143-1057290	223.3479	-3.7124	16.44	0.99		
PQSJ065746.22-014940.4	2MASS J06574621-0149400	215.2807	0.5748	18.97	0.88		
PQSJ065814.61+104757.8		204.0488	6.3958	19.06	0.15		
PQSJ065916.36+123132.1		202.6035	7.3880	18.84	1.09		
PQSJ070000.47+152252.3		200.0913	8.8024	18.06	1.39		
PQSJ070001.43+170922.3	ICRF J070001.5+170921	198.4730	9.5761	19.07	1.12	1.0800	2017ApJS..233....3T
PQSJ070139.60+083017.2		206.4924	6.1242	18.24	0.86		
PQSJ070240.89+114104.1	LAMOST J070240.89+114104.0	203.7361	7.7637	17.89	0.96		
PQSJ070302.13+155735.6		199.8836	9.7101	18.52	1.15		
PQSJ070331.29-252317.8		237.0179	-8.8083	19.35	1.37		
PQSJ070344.49+510042.8	2MASS J07034450+5100423	165.8196	22.6111	18.04	1.12		
PQSJ070418.57-065641.6	2MASS J07041857-0656417	220.5763	-0.3176	17.73	0.81		
PQSJ070518.98+061219.8		208.9676	5.9025	16.89	0.78		
PQSJ070529.39+633333.6	LEDA 138983	152.4659	25.6308	16.15	1.03	0.1530	1991ApJS...76..813S
PQSJ070713.20+643600.4	LEDA 20174	151.3597	25.9876	16.15	0.92	0.0795	2000ApJ...543..552S
PQSJ070836.02+131053.0		203.0160	9.7187	18.87	1.03		
PQSJ070903.38+093508.5		206.3365	8.2405	18.46	1.12		
PQSJ070919.27+254923.5	UVQS J070919.25+254923.4	191.3114	15.1338	16.82	0.88	0.1360	2016AJ....152...25M
PQSJ071113.13+544653.8	2MASS J07111316+5446533	162.1339	24.6306	17.63	0.99		
PQSJ071134.79+052347.0		210.4000	6.9299	19.26	1.31		
PQSJ071139.40-023737.5	2MASS J07113941-0237376	217.5815	3.2924	18.67	0.92		
PQSJ071156.40+070836.5		208.8658	7.7932	18.83	1.21		
PQSJ071216.93-832815.0		295.6722	-26.3488	18.39	1.31		
PQSJ071410.05+063322.3		209.6457	8.0252	18.73	1.12		
PQSJ071415.08+454156.3	Mrk 376	171.8771	22.8371	16.71	1.06	0.0560	2016AJ....152...25M
PQSJ071507.96+064235.2	1RXS J071508.3+064240	209.6152	8.3083	19.10	0.92		
PQSJ071708.06+004836.7		215.1468	6.0858	19.36	1.07		
PQSJ071800.67+440527.6	ATO J109.5025+44.0908	173.7551	23.0308	15.92	0.97	0.0634	2011MNRAS.416.2840L
PQSJ071825.04+194107.6		197.9989	14.5971	17.81	1.08		
PQSJ071831.03+084248.2		208.1743	9.9495	18.83	1.31		
PQSJ071938.07+542637.6	2MASS J07193801+5426372	162.7791	25.7520	17.73	0.94		
PQSJ071945.14+315347.3	ATO J109.9381+31.8962	186.2971	19.5148	17.42	0.97		
PQSJ071950.85+742757.0	QSO B0713+745	140.4417	27.9564	16.91	1.20	0.4750	2016ApJ...818..113N
PQSJ072001.62+181726.3	EM* StHA 62	199.4742	14.3736	14.19	0.96		
PQSJ072049.96-135134.1	2MASS J07204996-1351340	228.5853	0.0742	18.82	1.08		
PQSJ072051.14-021033.9	2MASS J07205117-0210335	218.2421	5.5386	18.01	0.90		
PQSJ072108.99-251033.6	IRAS 07191-2504	238.6349	-5.1548	18.03	0.56		
PQSJ072153.36+712036.2	8C 0716+714	143.9811	28.0176	15.10	1.00	0.3000	2016ApJ...818..113N
PQSJ072217.53+303050.5	LEDA 1906770	187.8728	19.5384	16.86	1.01	0.1000	2016AJ....152...25M
PQSJ072241.80+023436.8	2MASS J07224180+0234369	214.2009	8.1284	17.35	0.95		
PQSJ072331.84-014626.7	2MASS J07233186-0146267	218.1947	6.3178	18.53	1.15		
PQSJ072434.03-000558.5		216.8187	7.3200	18.39	0.94		
PQSJ072605.44-012730.9		218.2111	7.0310	19.02	1.13		
PQSJ072743.77-001418.2		217.3103	7.9579	17.60	1.22		
PQSJ072839.16+015905.6		215.4196	9.1831	19.13	1.33		
PQSJ073309.17+455506.5	2MASS J07330920+4555062	172.5508	26.0804	16.89	0.95	0.1414	2009ApJS..182..543A
PQSJ073359.63-041814.0		221.6760	7.4481	18.83	0.98		
PQSJ073405.87+135316.7	UVQS J073405.85+135316.7	205.0720	15.6250	17.11	1.06	0.3060	2016AJ....152...25M
PQSJ073623.17+392618.1	2MASX J07362309+3926173	179.6768	25.0625	16.60	0.97	0.1181	2009ApJS..182..543A

Table 1 *continued*

Table 1 *(continued)*

PQS Name	SIMBAD Name	l	b	m_{NUV}	W1−W2	Ref z	Ref
PQSJ073710.03-131133.7		229.8967	3.8809	18.57	1.03		
PQSJ073807.05+212730.6	2MASS J07380702+2127295	198.1950	19.5333	16.76	1.33	0.7520	2016AJ....152...25M
PQSJ073833.88-020423.1	3C 185	220.2272	9.5035	18.49	1.26	1.0330	2002LEDA.........0P
PQSJ073949.44+532314.4		164.5076	28.5057	17.47	1.15		
PQSJ074126.40+354703.0	2MASS J07412637+3547027	183.8584	25.0180	17.78	0.95	0.1328	2012AJ....143...64J
PQSJ074227.08+465643.0	LEDA 3095768	171.7961	27.8604	18.03	0.94	0.1678	2012ApJS..203...21A
PQSJ074232.82+494834.2	Mrk 79	168.6027	28.3822	15.67	1.08	0.0223	2015A&A...573A..59G
PQSJ074312.55+742936.8	2E 1852	140.3544	29.5169	17.33	0.99	0.3120	1991ApJS...76..813S
PQSJ074522.77-135543.3		231.5213	5.2602	17.20	0.61		
PQSJ074541.63+314256.7	ICRF J074541.6+314256	188.4296	24.6626	16.54	1.06	0.4609	2012ApJS..203...21A
PQSJ074552.29-080816.7		226.4996	8.2067	18.25	1.14		
PQSJ074706.93-113421.0		229.6714	6.7921	18.63	1.17		
PQSJ074906.53+451034.6	7C 074532.29+451808.00	174.0155	28.6613	17.04	1.02	0.1922	2018A&A...613A..51P
PQSJ074910.59+284214.5	2MASS J07491060+2842145	191.8329	24.4308	17.56	0.99	0.3440	2012ApJS..203...21A
PQSJ074948.30+345444.3	2MASS J07494826+3454439	185.3158	26.4127	17.25	0.94	0.1323	2012ApJS..203...21A
PQSJ074950.82+335743.9	IC 2207	186.3365	26.1569	17.63	0.75	0.0160	2015ApJS..219...12A
PQSJ075004.42+170244.7	2MASS J07500439+1702459	203.6865	20.4260	17.38	1.07	0.3683	2012ApJS..203...21A
PQSJ075051.06+775101.6		136.4612	29.5899	17.13	1.23		
PQSJ075100.75+032041.0	2MASX J07510082+0320401	216.7908	14.7715	15.72	1.00	0.0990	2002LEDA.........0P
PQSJ075112.30+291938.9	QSO B0748+295	191.3377	25.0497	16.30	1.28	0.9142	2012ApJS..203...21A
PQSJ075126.22+360949.3	2MASS J07512622+3609492	184.0651	27.0674	17.92	0.95	0.1482	2012ApJS..203...21A
PQSJ075225.74+283040.0	2MASS J07522573+2830399	192.2860	25.0451	17.50	0.61	0.0618	2012ApJS..203...21A
PQSJ075441.42+010149.7		219.3511	14.5180	17.63	1.19		
PQSJ075459.48-041918.9	2MASS J07545948-0419190	224.2267	12.0398	17.83	1.01		
PQSJ075525.29+391109.7	[OKM2018] SWIFT J0755.7+3912	180.9678	28.5683	16.09	0.69	0.0332	2012A&A...545A..15S
PQSJ075649.44-095349.9	SDSS J075649.43-095349.8	229.3978	9.6937	19.11	1.13		
PQSJ075706.65+095635.5	QSO B0754+10	211.3115	19.0571	17.10	1.10	0.2660	2011NewA...16..503M
PQSJ075730.37+152453.2	ATO J119.3765+15.4147	206.0476	21.4154	17.17	1.04	0.3886	2012ApJS..203...21A
PQSJ075800.07+392029.3	1E 0754+39.3	180.9215	29.0896	16.03	0.95	0.0950	2016AJ....152...25M
PQSJ075819.70+421934.7	LEDA 2196699	177.5812	29.7600	17.11	1.05	0.2112	2018A&A...613A..51P
PQSJ080136.82-063609.4	2MASS J08013683-0636095	227.0867	12.3608	17.65	0.75	0.0862	2009MNRAS.399..683J
PQSJ080405.93+050649.5	RC J0804+0506	216.6961	18.4817	16.93	1.39		
PQSJ080452.73+212049.6	LEDA 139051	200.7895	25.2831	16.86	0.99	0.1244	2012ApJS..203...21A
PQSJ080554.10+111432.8	2MASS J08055411+1114324	211.0375	21.5648	17.52	1.05	0.2274	2012ApJS..203...21A
PQSJ080627.14-211621.7		240.4401	5.8083	18.90	1.23		
PQSJ080634.87-283159.8	WRAY 15-157	246.6045	1.9475	18.95	1.07	0.0003	2018yCat.1345....0G
PQSJ080919.34-202653.8		240.0980	6.8151	18.32	1.19		
PQSJ080954.39+074355.6	2MASS J08095437+0743553	214.8929	20.9426	17.06	1.11	0.6521	2012ApJS..203...21A
PQSJ081028.70-165220.6		237.1895	8.9512	19.14	1.36		
PQSJ081119.31-180252.8		238.3050	8.4963	19.19	1.27		
PQSJ081303.50-205251.9		240.9393	7.3190	19.00	1.44		
PQSJ081459.52-181520.8		238.9557	9.1206	19.14	1.17		
PQSJ081522.96+015500.4	ICRF J081522.9+015459	221.0706	19.5006	17.24	1.11	0.4000	2017ApJS..233....3T
PQSJ081629.39-180906.8		239.0618	9.4761	18.99	1.01		
PQSJ081807.57+024932.2	UVQS J081807.53+024932.1	220.5604	20.5330	17.26	0.64	0.0630	2016AJ....152...25M
PQSJ082045.40+130618.7	[VV2000] J082045.4+130618	210.8302	25.6404	16.63	1.35	1.1248	2009ApJS..182..543A
PQSJ082347.03-201252.2		241.7693	9.7837	18.89	1.51		
PQSJ082559.42-135142.5	UVQS J082559.37-135142.7	236.6484	13.7220	17.43	1.11	0.3190	2016AJ....152...25M
PQSJ082628.22+085535.7	2MASS J08262820+0855354	215.6789	25.1486	17.73	1.02	0.2543	2009ApJS..182..543A
PQSJ082633.57+074248.3	QSO J0826+0742	216.8905	24.6344	17.37	1.08	0.3113	2012ApJS..203...21A
PQSJ082930.52+081238.3	LEDA 1341762	216.7553	25.5093	17.33	1.04	0.1291	2009ApJS..182..543A
PQSJ083011.01-250252.0		246.6490	8.2618	18.78	1.29		
PQSJ083016.49-672528.6	2MASX J08301655-6725289	281.6422	-16.1542	16.96	0.69	0.0348	2009MNRAS.399..683J
PQSJ083029.00+024304.1	2MASS J08302893+0243038	222.2342	23.2014	17.74	1.00		

Table 1 *continued*

Table 1 *(continued)*

PQS Name	SIMBAD Name	*l*	*b*	m_{NUV}	W1−W2	Ref z	Ref
PQSJ083356.46-010113.0	6dFGS gJ083356.5-010112	226.2272	22.1314	16.49	1.20	0.2907	2009MNRAS.399..683J
PQSJ083452.34-233540.1		246.0759	9.9743	18.87	0.91		
PQSJ083641.49-040808.7		229.4885	21.1372	17.57	1.20		
PQSJ083752.29-244028.5		247.3715	9.8962	18.82	1.24		
PQSJ084219.12-034931.4	2MASS J08421910-0349314	229.9894	22.4972	17.11	1.19	0.3566	2009MNRAS.399..683J
PQSJ084320.25-264017.3	2MASS J08432025-2640177	249.7434	9.6936	18.40	1.26		
PQSJ084553.53-024100.2	[VV2006] J084553.4-024100	229.4348	23.8535	16.64	1.10	0.4680	2018AJ....155..189D
PQSJ085259.18+031320.4	2MASS J08525922+0313207	224.7534	28.3666	17.33	1.03	0.2968	2012ApJS..203...21A
PQSJ085506.79-030336.5	2MASS J08550679-0303368	231.1207	25.6137	17.67	0.98		
PQSJ085915.68+011800.4	2MASS J08591566+0118006	227.5403	28.7681	17.72	1.03	0.2821	2012ApJS..203...21A
PQSJ090420.87+013038.4	[VV2006] J090420.9+013038	228.0758	29.9692	17.19	1.27	0.7921	2012ApJS..203...21A
PQSJ090553.67-042612.3	2MASS J09055360-0426119	234.0405	27.1257	16.46	1.05	0.3700	2016AJ....152...25M
PQSJ091134.96-134801.4	2MASS J09113489-1348022	243.3322	22.7939	17.93	1.07		
PQSJ091945.29-063225.5	2MASS J09194530-0632252	238.2226	28.7612	16.65	1.02	0.7061	2009MNRAS.399..683J
PQSJ092100.39-051545.7	2MASS J09210036-0515465	237.2411	29.7594	17.36	1.06	0.3800	2016AJ....152...25M
PQSJ092101.13-134252.0		244.8115	24.6442	18.82	1.07		
PQSJ092233.99-124225.6		244.2060	25.5694	18.55	1.14		
PQSJ092315.05-132826.5	1RXS J092315.2-132817	244.9822	25.2169	18.18	0.76		
PQSJ092443.26-130344.2		244.8787	25.7543	18.76	1.36		
PQSJ092751.79-203451.5	ICRF J092751.8-203451	251.6378	21.4229	16.76	1.04	0.3474	2009MNRAS.399..683J
PQSJ092815.22-122132.6		244.8797	26.8664	18.85	1.13		
PQSJ093318.16-171440.3	[VV2006] J093318.1-171441	249.8788	24.6114	17.66	1.19	0.3100	2000ApJS..129..547B
PQSJ093622.14-113433.9	2MASS J09362212-1134342	245.6347	28.8930	17.78	0.75	0.0912	2009MNRAS.399..683J
PQSJ093846.25-215547.5	2MASS J09384620-2155477	254.5713	22.3549	15.73	1.06	0.2487	2009MNRAS.399..683J
PQSJ093911.30-111145.7	2MASS J09391128-1111454	245.8140	29.6659	17.59	0.99		
PQSJ094745.72-215547.6	[VV96] J094745.8-215547	256.1721	23.8313	17.53	1.24	0.3160	2016AJ....152...25M
PQSJ095513.58-212303.1	LEDA 828986	257.1338	25.4255	17.22	0.67	0.1085	2009MNRAS.399..683J
PQSJ095912.22-185250.1	EC 09568-1838	255.9711	27.8872	16.06	1.23	0.5720	2016AJ....152...25M
PQSJ100159.80-443802.0	QSO B0959-443	273.9334	8.4888	17.77	1.24	0.8370	1989ApJS...69....1H
PQSJ100826.52-273544.3	2MASS J10082651-2735443	264.0898	22.7249	17.00	1.06	0.3080	2016AJ....152...25M
PQSJ102239.94-302930.6	2MASS J10223994-3029305	268.6664	22.3055	17.40	1.07	0.3165	2009MNRAS.399..683J
PQSJ102542.52-265349.9	1RXS J102542.9-265354	266.9630	25.6138	17.74	0.93		
PQSJ103126.83-273959.2		268.6109	25.7201	18.34	1.11		
PQSJ103236.07-281326.9	QSO B1030-2757	269.1928	25.4032	16.37	1.06	0.1484	2009MNRAS.399..683J
PQSJ104833.80-390237.8	2MASS J10483382-3902379	278.2949	17.8787	16.82	0.88	0.0450	2016AJ....152...25M
PQSJ105251.04-272716.1	HE 1050-2711	272.9878	28.4336	16.49	0.99	0.2070	2016AJ....152...25M
PQSJ105727.86-403940.5	6dFGS gJ105727.9-403941	280.6670	17.2315	17.35	1.03	0.3981	2009MNRAS.399..683J
PQSJ110106.88-303605.7	EC 10587-3019	276.4788	26.5423	16.73	1.07	0.3257	2009MNRAS.399..683J
PQSJ110331.56-325116.7	CTS 10	278.1173	24.7652	16.91	1.10	0.3555	2009MNRAS.399..683J
PQSJ111028.89-603155.9	2MASS J11102887-6031558	290.8237	-0.0558	18.24	0.61	0.0000	2020AJ....160..120J
PQSJ111704.03-290230.5	CTS 11	279.2387	29.4519	16.88	1.03	0.0700	2016AJ....152...25M
PQSJ112048.59-293939.3	EC 11183-2923	280.3805	29.2117	17.34	1.25		
PQSJ112731.83-304445.6	HE 1125-3028	282.3863	28.7563	16.71	1.27	0.6680	2016AJ....152...25M
PQSJ112855.15-343214.0		284.2046	25.3158	17.75	0.97		
PQSJ112914.99-383730.3	2MASS J11291493-3837306	285.7926	21.4958	17.00	0.96	0.2328	2009MNRAS.399..683J
PQSJ114755.66-385809.3		289.6448	22.2583	17.40	1.13		
PQSJ115227.68-374837.7	2MASS J11522769-3748378	290.2564	23.6053	17.80	1.05		
PQSJ121514.39-322101.8	2MASS J12151434-3221016	294.1150	29.9007	17.68	0.99		
PQSJ123137.19-475802.5	2MASX J12313717-4758019	299.5034	14.7724	16.41	0.82	0.0279	2009MNRAS.399..683J
PQSJ130421.04-435310.5	2MASS J13042100-4353102	305.3909	18.9238	16.91	0.86		
PQSJ130809.02-455417.0	2MASS J13080899-4554180	305.9687	16.8685	17.28	1.05	0.3320	2016AJ....152...25M
PQSJ132225.68-325431.3		310.4045	29.5130	16.25	0.62		
PQSJ133325.99-340052.8	ESO 383-18	312.7862	28.0522	17.06	1.31	0.0130	2004MNRAS.355..273C
PQSJ140806.74-302354.3	2MAXI J1406-300	321.9462	29.6266	16.53	1.04	0.0250	2016AJ....152...25M

Table 1 *continued*

Table 1 *(continued)*

PQS Name	SIMBAD Name	l	b	m_{NUV}	W1−W2	Ref z	Ref
PQSJ152052.55-213358.3	2MASS J15205249-2133581	343.2845	29.3584	17.45	1.06	0.1502	2009MNRAS.399..683J
PQSJ152546.60-235430.2		342.6406	26.8207	18.61	1.06		
PQSJ160551.09-611144.5	LEDA 3079933	324.2714	-6.6615	18.79	0.81	0.0520	2008A&A...482..113M
PQSJ161836.16-592716.5	LEDA 3078020	326.6297	-6.4847	18.76	0.69	0.0356	2011MNRAS.416.2840L
PQSJ162526.51+852941.9	LEDA 58086	118.7615	29.7461	17.47	0.85	0.0629	2002LEDA.........0P
PQSJ164533.35+022059.6	UVQS J164533.31+022059.3	19.6376	28.8772	16.83	1.15	0.6450	2016AJ....152...25M
PQSJ165605.59-520340.3	2MASS J16560561-5203408	335.6882	-5.4921	18.52	0.98	0.0540	2006A&A...459...21M
PQSJ170025.18-724044.7	2MASS J17002537-7240450	319.0313	-18.1745	17.65	0.86	0.1047	2009MNRAS.399..683J
PQSJ172421.73+063837.9	2MASX J17242174+0638371	28.9010	22.3712	16.97	0.79	0.0220	2016AJ....152...25M
PQSJ172422.82-513410.1		338.6679	-8.7477	18.83	1.38		
PQSJ173840.53+322409.2	7C 173649.10+322532.00	56.9083	28.6152	16.90	0.91	0.1300	2017ApJS..233....3T
PQSJ174128.11+034852.0	IRAS 17389+0350	28.2732	17.2928	17.53	1.17	0.0230	2016AJ....152...25M
PQSJ174206.89+182721.1	4C 18.51	42.5163	23.3181	17.24	1.00	0.1860	2016ApJ...818..113N
PQSJ174506.56-020843.7		23.2521	13.6946	18.02	1.04		
PQSJ174638.78+411047.3	2MASS J17463884+4110467	67.0808	29.1495	17.27	1.01		
PQSJ174704.02+260336.2	LAMOST J174704.02+260337.0	50.7509	24.9571	18.43	1.02	0.3403	2018AJ....155..189D
PQSJ174707.17+383519.4		64.2172	28.4954	17.71	1.03		
PQSJ175044.52+255518.0	SDSS J175044.50+255518.1	50.9117	24.1326	18.47	1.03	0.3900	2018AJ....155..189D
PQSJ175114.15+253931.5		50.6821	23.9389	18.94	1.30		
PQSJ180055.04+423957.1	2MASS J18005509+4239572	69.3756	26.8802	17.14	0.99		
PQSJ180249.59+512007.5		79.0442	28.2356	17.45	1.02		
PQSJ180650.80+694928.4	3C 371	100.1314	29.1668	17.07	0.86	0.0510	2016AJ....152...25M
PQSJ181234.59+395126.5	2MASS J18123455+3951260	66.9813	24.0494	17.25	1.01		
PQSJ181828.96+674125.6	2E 4057	97.7368	28.0517	16.45	1.03	0.3140	2004ApJ...617..192M
PQSJ182211.47-700219.2	UVQS J182211.57-700219.5	324.5067	-22.9496	17.84	1.17	0.3530	2016AJ....152...25M
PQSJ182408.93+464017.1	LEDA 165770	74.7816	23.8437	16.95	0.83	0.0696	2011MNRAS.416.2840L
PQSJ182446.44+650924.7	HS 1824+6507	94.9492	27.2062	17.21	1.11	0.3000	1995A&A...300..323J
PQSJ182754.15+095853.6	LS IV +09 4	39.2359	9.7234	14.83	0.74		
PQSJ183023.19+731310.6	2MASS J18302317+7313107	104.0389	27.3960	14.67	0.96	0.1230	2001AJ....121.2843B
PQSJ183046.48+094459.2		39.3408	8.9862	19.79	0.89		
PQSJ183249.71+534021.8	LEDA 2447627	82.5863	24.2128	17.12	0.64	0.0390	2016ApJ...818..113N
PQSJ183503.36+324146.5	ICRF J183503.3+324146	61.3051	17.4461	15.71	0.94	0.0581	2002LEDA.........0P
PQSJ183849.18+480234.4	ATO J279.7048+48.0428	76.9498	21.8289	17.21	0.73	0.3000	2013MNRAS.430.2464M
PQSJ184640.81+635128.7	UVQS J184640.72+635128.5	93.9346	24.6757	17.25	1.19	0.4080	2016AJ....152...25M
PQSJ185700.07+160626.6	2MASS J18570009+1606261	47.9428	6.0707	19.39	0.77		
PQSJ185801.14+485023.3	1RXS J185800.9+485020	78.8222	19.0554	17.69	0.86	0.0790	2012ApJ...751...52E
PQSJ190525.86+422739.2	Z 229-15	73.0896	15.5315	17.76	0.70	0.0275	2002LEDA.........0P
PQSJ190938.94-622854.5	ESO 104-41	333.7333	-25.9149	16.70	0.96	0.0852	2009MNRAS.399..683J
PQSJ191928.08-295808.3	LEDA 2829969	8.1819	-18.7741	16.00	1.05	0.1668	2009MNRAS.399..683J
PQSJ192114.11-584013.4	ESO 141-55	338.1833	-26.7111	14.61	0.87	0.0371	2009MNRAS.399..683J
PQSJ192447.35-512427.3	UVQS J192447.29-512426.4	346.2566	-25.9062	16.44	1.20	0.7660	2016AJ....152...25M
PQSJ192933.39-390841.9	UVQS J192933.41-390842.1	359.5861	-23.7113	17.62	1.08	0.4230	2016AJ....152...25M
PQSJ193008.30+020449.4		39.2395	-7.6383	19.36	1.33		
PQSJ193423.21-515129.4	UVQS J193423.24-515129.8	346.0735	-27.4535	18.06	1.14	0.1690	2016AJ....152...25M
PQSJ193804.21-510949.3	2MASS J19380439-5109493	346.9551	-27.9020	16.32	0.70	0.0400	2009MNRAS.399..683J
PQSJ193810.75+540856.0		86.4448	15.3090	17.55	1.10		
PQSJ193819.64-432645.9	2MASS J19381959-4326461	355.4683	-26.4134	16.28	1.02	0.0791	2009MNRAS.399..683J
PQSJ193929.56+700748.8	2MASS J19392938+7007490	102.0032	21.4616	17.30	1.00	0.1200	2016ApJ...818..113N
PQSJ194357.73-140911.5	NGC 6818	25.8586	-17.9112	12.92	1.87	-0.0000	1953GCRV..C......0W
PQSJ194545.28-474735.1		350.9649	-28.5639	17.71	1.01		
PQSJ194635.31+041727.5		43.1722	-10.2178	17.48	0.71		
PQSJ194658.72+052021.8	1RXS J194658.6+052031	44.1538	-9.8004	19.88	1.10		
PQSJ194732.38-421750.0	UVQS J194732.37-421750.0	357.1506	-27.8012	17.11	1.02	0.2420	2016AJ....152...25M
PQSJ195041.28-200021.6	UVQS J195041.29-200021.6	20.8204	-21.7034	17.09	0.97	0.2920	2016AJ....152...25M

Table 1 *continued*

Table 1 *(continued)*

PQS Name	SIMBAD Name	l	b	m_{NUV}	W1−W2	Ref z	Ref
PQSJ195904.13+105335.5		50.5527	-9.6715	18.86	1.32		
PQSJ200631.82-153906.5	IRAS 20037-1547	26.7465	-23.5041	17.80	1.00	0.1919	2011MNRAS.414..500H
PQSJ202202.37-182259.9	2MASX J20220235-1822587	25.5130	-27.9729	17.53	0.77	0.0549	2009MNRAS.399..683J
PQSJ202610.07+112928.0	2MASS J20261004+1129279	54.6127	-15.0388	17.04	0.99		
PQSJ203202.53-102330.9	2MASS J20320251-1023314	34.8669	-27.0196	17.85	0.91		
PQSJ203311.82+173234.1	UVQS J203311.76+173234.0	60.7865	-13.1253	17.22	1.03	0.2340	2016AJ....152...25M
PQSJ203335.87-032038.6	2MASS J20333589-0320385	42.0361	-24.1831	17.07	1.07	0.6960	2016AJ....152...25M
PQSJ203413.30-040529.0	LEDA 1062999	41.3933	-24.6733	16.52	0.84		
PQSJ204237.21+750802.1	ICRF J204237.3+750802	108.9977	19.5267	17.23	0.99	0.1040	2002LEDA.........0P
PQSJ204303.53-010125.0	[VV2006] J204303.6-010126	45.5299	-25.1254	18.35	1.43	1.1899	2009ApJS..182..543A
PQSJ204306.26+032451.4	2MASS J20430626+0324516	49.7200	-22.8787	17.47	1.13	0.2710	1995A&AS..110..469B
PQSJ204409.71-104324.3	Mrk 509	35.9711	-29.8550	14.50	0.89	0.0350	2016ApJ...818..113N
PQSJ204620.87-024845.2	Mrk 896	44.2456	-26.7197	16.36	0.66	0.0268	2011MNRAS.416.2840L
PQSJ205256.03+024546.2		50.5220	-25.3097	16.88	0.89		
PQSJ205820.58+340138.6		77.5978	-7.6261	18.62	1.31		
PQSJ210931.91+353258.5	ICRF J210931.8+353257	80.2819	-8.3528	17.44	0.99	0.2015	2013ApJ...767...14P
PQSJ211420.95+252422.9	ATO J318.5876+25.4062	73.2535	-15.8905	17.50	1.13		
PQSJ211452.57+060742.9	2MASS J21145258+0607423	57.0403	-28.0144	16.58	1.20	0.4570	2017AJ....154..114O
PQSJ211547.08+190843.0	[VV2000] J211547.1+190843	68.4845	-20.2226	16.79	1.20	0.4100	2016AJ....152...25M
PQSJ214153.44+315127.1	2MASX J21415350+3151282	82.4352	-15.7309	17.55	0.66	0.0433	2002LEDA.........0P
PQSJ214335.53+174349.4	ICRF J214335.5+174348	72.1156	-26.0841	16.92	1.11	0.2130	2016ApJ...818..113N
PQSJ215647.45+224250.2	QSO J2156+2242	78.4262	-24.6981	15.97	1.24	1.2900	2016ApJ...818..113N
PQSJ220314.97+314538.5	4C 31.63	85.9568	-18.7787	16.24	1.03	0.2970	2016ApJ...818..113N
PQSJ220651.79+275758.6	2MASS J22065183+2757584	84.0498	-22.2169	17.24	1.01		
PQSJ221536.83+290235.4	4C 28.53	86.4035	-22.5622	16.69	1.02	0.2290	1999A&AS..139..575W
PQSJ223954.44+272431.9	LEDA 1807248	90.1932	-26.9743	17.38	0.94	0.0654	2020ApJS..250....8L
PQSJ224436.88+475301.3	1RXS J224436.9+475306	101.9768	-9.7610	18.83	1.28		
PQSJ225147.70+341930.6	LEDA 3096705	96.4956	-22.3319	17.42	1.02	0.1320	1999A&AS..139..575W
PQSJ225603.39+273209.7	HS 2253+2716	93.7370	-28.7147	17.07	1.18	0.3635	2020ApJS..250....8L
PQSJ232026.52+592924.3	IRAS 23182+5912	111.6068	-1.3658	19.23	1.01		
PQSJ234229.32+530025.5	2MASS J23422932+5300254	112.5463	-8.4685	19.23	1.02		
PQSJ235217.32+332329.9	LEDA 2031036	108.9824	-27.8727	17.55	0.93		

Note— Properties of Plane QSO candidates, including their PQS and SIMBAD names, their Galactic coordinates, their GALEX NUV magnitudes, and W1-W2 colors. 165 of these 305 PQS QSO candidates have spectroscopic redshifts available in the literature, and the last two columns of this table list the published redshifts and their sources, when available.

Table 2. Plane QSO Candidate Spectroscopic Redshifts

PQS Name	l	b	m_{NUV}	Telescope	Type	z_{narrow}	z_{MARZ}	Ref z	Ref
PQSJ002324.76+605103.6	119.5240	-1.8350	16.50	APO-3.5m	Star		0.0000		
PQSJ004342.52+372520.1	121.2328	-25.4239	16.74	MDM-2.4m	AGN	0.0797	0.0801	0.0800	2015RAA....15.1438H
PQSJ004818.93+394112.1	122.2785	-23.1810	16.71	APO-3.5m	AGN	0.1349	0.1349	0.1340	2016ApJ...818..113N
PQSJ005050.78+353644.0	122.7967	-27.2593	16.47	MDM-2.4m	AGN	0.0581	0.0583	0.0580	2016AJ....152...25M
PQSJ010131.18+422935.1	124.9137	-20.3397	16.94	APO-3.5m	AGN	0.1848	0.1850	0.1900	2016ApJ...818..113N
PQSJ010415.84+402243.5	125.5740	-22.4271	16.50	APO-3.5m	AGN	0.1920	0.1926	0.1910	2016AJ....152...25M
PQSJ011745.63+363714.6	128.8032	-25.9506	17.51	MDM-2.4m	AGN	0.1058	0.1062	0.1100	2015RAA....15.1438H
PQSJ011849.46+383618.8	128.7829	-23.9551	17.92	APO-3.5m	AGN	0.2157	0.2162	0.2200	2015RAA....15.1438H
PQSJ012400.58+410709.9	129.5100	-21.3358	17.57	APO-3.5m	AGN	0.3465	0.3490		
PQSJ013925.09+370454.9	133.4563	-24.8072	17.39	APO-3.5m	AGN	0.1439	0.1440		

Table 2 *continued*

Table 2 *(continued)*

PQS Name	l	b	m_{NUV}	Telescope	Type	z_{narrow}	z_{MARZ}	Ref z	Ref
PQSJ021248.58+330643.3	141.9604	-26.7352	17.69	APO-3.5m	AGN	0.1883	0.1887		
PQSJ021935.13+534019.9	135.8717	-6.9702	17.26	APO-3.5m	AGN		0.0005		
PQSJ031304.24+461120.7	146.9644	-9.9689	19.75	APO-3.5m	Star		0.0000		
PQSJ031409.36+471111.0	146.5947	-9.0222	18.82	APO-3.5m	AGN		1.2919		
PQSJ032839.48+451440.5	149.7976	-9.2689	20.14	APO-3.5m	AGN	0.1038	0.1044		
PQSJ040821.86+604649.4	144.7800	6.5612	19.74	APO-3.5m	Star		0.0000		
PQSJ052113.09+802100.9	132.6207	23.0984	17.23	APO-3.5m	AGN	0.2623	0.2627		
PQSJ053715.36+345344.8	174.0027	1.6442	18.29	APO-3.5m	Star		0.0000		
PQSJ055425.29-280544.8	233.4567	-24.0828	16.65	APO-3.5m	AGN		0.0626	0.0630	2016AJ....152...25M
PQSJ060105.70-261108.9	232.0496	-22.0393	16.47	APO-3.5m	AGN	0.0390	0.0389	0.0390	2009MNRAS.399..683J
PQSJ063117.46-290730.7	237.5212	-16.8695	18.45	APO-3.5m	Star		0.0000		
PQSJ064011.77-255342.1	235.2352	-13.7918	17.23	APO-3.5m	AGN		0.0256	0.0258	2009MNRAS.399..683J
PQSJ065030.88-195929.0	230.7776	-9.1639	18.59	APO-3.5m	Star		0.0000	0.0258	2002LEDA.........0P
PQSJ072108.99-251033.6	238.6349	-5.1548	18.03	APO-3.5m	Star		0.0000		
PQSJ074522.77-135543.3	231.5213	5.2602	17.20	APO-3.5m	Star		0.0000		
PQSJ080919.34-202653.8	240.0980	6.8151	18.32	APO-3.5m	AGN		0.5304		
PQSJ082559.42-135142.5	236.6484	13.7220	17.43	APO-3.5m	AGN	0.3194	0.3199	0.3190	2016AJ....152...25M
PQSJ084320.25-264017.3	249.7434	9.6936	18.40	APO-3.5m	AGN		0.6495		
PQSJ085506.79-030336.5	231.1207	25.6137	17.67	APO-3.5m	AGN	0.2689	0.2694		
PQSJ091134.96-134801.4	243.3322	22.7939	17.93	APO-3.5m	AGN	0.2171	0.2167		
PQSJ091945.29-063225.5	238.2226	28.7612	16.65	APO-3.5m	AGN	0.7066	0.7068	0.7061	2009MNRAS.399..683J
PQSJ092100.39-051545.7	237.2411	29.7594	17.36	APO-3.5m	AGN		0.3804	0.3800	2016AJ....152...25M
PQSJ092315.05-132826.5	244.9822	25.2169	18.18	APO-3.5m	AGN	0.1877	0.1876		
PQSJ092751.79-203451.5	251.6378	21.4229	16.76	APO-3.5m	Star		0.0000	0.3474	2009MNRAS.399..683J
PQSJ093622.14-113433.9	245.6347	28.8930	17.78	APO-3.5m	AGN	0.0912	0.0917	0.0912	2009MNRAS.399..683J
PQSJ100826.52-273544.3	264.0898	22.7249	17.00	APO-3.5m	AGN	0.3071	0.3081	0.3080	2016AJ....152...25M
PQSJ102239.94-302930.6	268.6664	22.3055	17.40	APO-3.5m	AGN	0.3165	0.3168	0.3165	2009MNRAS.399..683J
PQSJ110331.56-325116.7	278.1173	24.7652	16.91	APO-3.5m	AGN	0.3554	0.3557	0.3555	2009MNRAS.399..683J
PQSJ162526.51+852941.9	118.7615	29.7461	17.47	APO-3.5m	AGN	0.0631	0.0634	0.0629	2002LEDA.........0P
PQSJ173840.53+322409.2	56.9083	28.6152	16.90	MDM-1.3m	AGN	0.1273	0.1278	0.1300	2017ApJS..233....3T
PQSJ174638.78+411047.3	67.0808	29.1495	17.27	MDM-1.3m	AGN	0.3008	0.3010		
PQSJ174704.02+260336.2	50.7509	24.9571	18.43	MDM-2.4m	AGN	0.3416	0.3422	0.3403	2018AJ....155..189D
PQSJ174707.17+383519.4	64.2172	28.4954	17.71	APO-3.5m	AGN	0.1338	0.1345		
PQSJ175044.52+255518.0	50.9117	24.1326	18.47	MDM-2.4m	AGN		0.3899	0.3900	2018AJ....155..189D
PQSJ180055.04+423957.1	69.3756	26.8802	17.14	MDM-1.3m	AGN	0.1691	0.1694		
PQSJ180650.80+694928.4	100.1314	29.1668	17.07	MDM-2.4m	AGN	0.0506	0.0518	0.0510	2016AJ....152...25M
PQSJ181234.59+395126.5	66.9813	24.0494	17.25	MDM-1.3m	AGN	0.2420	0.2422		
PQSJ181828.96+674125.6	97.7368	28.0517	16.45	MDM-1.3m	AGN	0.3128	0.3132	0.3140	2004ApJ...617..192M
PQSJ182408.93+464017.1	74.7816	23.8437	16.95	MDM-2.4m	AGN	0.0670	0.0675	0.0696	2011MNRAS.416.2840L
PQSJ182446.44+650924.7	94.9492	27.2062	17.21	MDM-2.4m	AGN	0.3044	0.3046	0.3000	1995A&A...300..323J
PQSJ183023.19+731310.6	104.0389	27.3960	14.67	APO-3.5m	AGN		0.1240	0.1230	2001AJ....121.2843B
PQSJ183249.71+534021.8	82.5863	24.2128	17.12	MDM-2.4m	AGN	0.0457	0.0459	0.0390	2016ApJ...818..113N
PQSJ183503.36+324146.5	61.3051	17.4461	15.71	MDM-2.4m	AGN	0.0587	0.0591	0.0581	2002LEDA.........0P
PQSJ183849.18+480234.4	76.9498	21.8289	17.21	MDM-2.4m	Star		0.0000	0.3000	2013MNRAS.430.2464M
PQSJ184640.81+635128.7	93.9346	24.6757	17.25	APO-3.5m	AGN	0.4081	0.4087	0.4080	2016AJ....152...25M
PQSJ185801.14+485023.3	78.8222	19.0554	17.69	APO-3.5m	AGN	0.0787	0.0790	0.0790	2012ApJ...751...52E
PQSJ190525.86+422739.2	73.0896	15.5315	17.76	APO-3.5m	AGN	0.0277	0.0280	0.0275	2002LEDA.........0P
PQSJ193008.30+020449.4	39.2395	-7.6383	19.36	APO-3.5m	Star		0.0000		
PQSJ193810.75+540856.0	86.4448	15.3090	17.55	APO-3.5m	AGN	0.2726	0.2731		
PQSJ193929.56+700748.8	102.0032	21.4616	17.30	MDM-2.4m	AGN	0.1161	0.1163	0.1200	2016ApJ...818..113N
PQSJ194635.31+041727.5	43.1722	-10.2178	17.48	APO-3.5m	Star		0.0000		
PQSJ202610.07+112928.0	54.6127	-15.0388	17.04	APO-3.5m	AGN	0.0861	0.0864		
PQSJ203311.82+173234.1	60.7865	-13.1253	17.22	APO-3.5m	AGN	0.2350	0.2357	0.2340	2016AJ....152...25M
PQSJ203413.30-040529.0	41.3933	-24.6733	16.52	APO-3.5m	AGN	0.1004	0.1010		

Table 2 *continued*

Table 2 *(continued)*

PQS Name	l	b	m_{NUV}	Telescope	Type	z_{narrow}	z_{MARZ}	Ref z	Ref
PQSJ204237.21+750802.1	108.9977	19.5267	17.23	APO-3.5m	AGN	0.1042	0.1041	0.1040	2002LEDA.........0P
PQSJ205256.03+024546.2	50.5220	-25.3097	16.88	MDM-2.4m	AGN	0.3613	0.3610		
PQSJ205820.58+340138.6	77.5978	-7.6261	18.62	APO-3.5m	AGN		0.9004		
PQSJ210931.91+353258.5	80.2819	-8.3528	17.44	APO-3.5m	AGN	0.2019	0.2023	0.2015	2013ApJ...767...14P
PQSJ211420.95+252422.9	73.2535	-15.8905	17.50	APO-3.5m	AGN	0.0890	0.0893		
PQSJ211452.57+060742.9	57.0403	-28.0144	16.58	MDM-2.4m	AGN		0.4608	0.4570	2017AJ....154..114O
PQSJ211547.08+190843.0	68.4845	-20.2226	16.79	APO-3.5m	AGN	0.4118	0.4120	0.4100	2016AJ....152...25M
PQSJ214153.44+315127.1	82.4352	-15.7309	17.55	APO-3.5m	AGN	0.0433	0.0436	0.0433	2002LEDA.........0P
PQSJ214335.53+174349.4	72.1156	-26.0841	16.92	MDM-2.4m	AGN	0.2105	0.2112	0.2130	2016ApJ...818..113N
PQSJ215647.45+224250.2	78.4262	-24.6981	15.97	APO-3.5m	AGN		1.3029	1.2900	2016ApJ...818..113N
PQSJ220314.97+314538.5	85.9568	-18.7787	16.24	APO-3.5m	AGN	0.2949	0.2954	0.2970	2016ApJ...818..113N
PQSJ220651.79+275758.6	84.0498	-22.2169	17.24	MDM-2.4m	AGN	0.2529	0.2528		
PQSJ221536.83+290235.4	86.4035	-22.5622	16.69	MDM-2.4m	AGN	0.2289	0.2293	0.2290	1999A&AS..139..575W
PQSJ223954.44+272431.9	90.1932	-26.9743	17.38	APO-3.5m	AGN	0.0650	0.0656	0.0654	2020ApJS..250....8L
PQSJ224436.88+475301.3	101.9768	-9.7610	18.83	APO-3.5m	AGN		0.8993		
PQSJ225147.70+341930.6	96.4956	-22.3319	17.42	MDM-2.4m	AGN	0.1318	0.1322	0.1320	1999A&AS..139..575W
PQSJ225603.39+273209.7	93.7370	-28.7147	17.07	APO-3.5m	AGN	0.3632	0.3641	0.3635	2020ApJS..250....8L
PQSJ234229.32+530025.5	112.5463	-8.4685	19.23	APO-3.5m	AGN	0.1520	0.1524		

Note—PQS candidates for which we obtained APO or MDM spectra. In addition to their PQS name, Galactic longtitude and latitude, and NUV magnitude, we provide the name of the telescope at which the data were taken, the spectral classification (either Star or AGN). We provide two redshift estimates for the confirmed AGN when possible: (1) z_{narrow} is estimated based on any narrow emission lines present in the spectrum, typically [OIII] $\lambda\lambda$ 4960, 5008. (2) z_{MARZ} is the redshift based on QSO template fitting by the Manual and Automated Redshifting Software (Hinton et al. 2016) or MARZ. When available, we also list previously published spectroscopic redshifts for the candidates, along with their sources.

REFERENCES

Abazajian, K. N., Adelman-McCarthy, J. K., Agüeros, M. A., et al. 2009, ApJS, 182, 543, doi: 10.1088/0067-0049/182/2/543

Ahn, C. P., Alexandroff, R., Allende Prieto, C., et al. 2012, ApJS, 203, 21, doi: 10.1088/0067-0049/203/2/21

Alam, S., Albareti, F. D., Allende Prieto, C., et al. 2015, ApJS, 219, 12, doi: 10.1088/0067-0049/219/1/12

Ashley, T., Fox, A. J., Cashman, F. H., et al. 2022, Nature Astronomy, 6, 968, doi: 10.1038/s41550-022-01720-0

Bade, N., Fink, H. H., Engels, D., et al. 1995, A&AS, 110, 469

Barkhouse, W. A., & Hall, P. B. 2001, AJ, 121, 2843, doi: 10.1086/320377

Bauer, F. E., Condon, J. J., Thuan, T. X., & Broderick, J. J. 2000, ApJS, 129, 547, doi: 10.1086/313425

Bish, H. V., Werk, J. K., Peek, J., Zheng, Y., & Putman, M. 2021, ApJ, 912, 8, doi: 10.3847/1538-4357/abeb6b

Bordoloi, R., Fox, A. J., Lockman, F. J., et al. 2017, ApJ, 834, 191, doi: 10.3847/1538-4357/834/2/191

Boroson, T. 2005, AJ, 130, 381, doi: 10.1086/431722

Bregman, J. N., Anderson, M. E., Miller, M. J., et al. 2018, ApJ, 862, 3, doi: 10.3847/1538-4357/aacafe

Buder, S., Asplund, M., Duong, L., et al. 2018, MNRAS, 478, 4513, doi: 10.1093/mnras/sty1281

Carretti, E., Crocker, R. M., Staveley-Smith, L., et al. 2013, Nature, 493, 66, doi: 10.1038/nature11734

Cid Fernandes, R., Gu, Q., Melnick, J., et al. 2004, MNRAS, 355, 273, doi: 10.1111/j.1365-2966.2004.08321.x

Cutri, R. M., Wright, E. L., Conrow, T., et al. 2021, VizieR Online Data Catalog, II/328

Dong, X. Y., Wu, X.-B., Ai, Y. L., et al. 2018, AJ, 155, 189, doi: 10.3847/1538-3881/aab5ae

D'Onghia, E., & Fox, A. J. 2016, ARA&A, 54, 363, doi: 10.1146/annurev-astro-081915-023251

Edelson, R., & Malkan, M. 2012, ApJ, 751, 52, doi: 10.1088/0004-637X/751/1/52

Flesch, E. W. 2023, The Open Journal of Astrophysics, 6, 49, doi: 10.21105/astro.2308.01505

Fraternali, F., & Binney, J. J. 2008, MNRAS, 386, 935, doi: 10.1111/j.1365-2966.2008.13071.x

Gaia Collaboration. 2018, VizieR Online Data Catalog: Gaia DR2 (Gaia Collaboration, 2018), VizieR On-line Data Catalog: I/345. Originally published in: 2018A&A...616A...1G; doi:10.5270/esa-ycs, doi: 10.26093/cds/vizier.1345

García-Lorenzo, B., Márquez, I., Barrera-Ballesteros, J. K., et al. 2015, A&A, 573, A59, doi: 10.1051/0004-6361/201423485

Haffner, L. M., Reynolds, R. J., Tufte, S. L., et al. 2003, ApJS, 149, 405, doi: 10.1086/378850

Hagen, H. J., Engels, D., & Reimers, D. 1999, A&AS, 134, 483, doi: 10.1051/aas:1999442

Haynes, M. P., Giovanelli, R., Kent, B. R., et al. 2018, ApJ, 861, 49, doi: 10.3847/1538-4357/aac956

Hernán-Caballero, A., & Hatziminaoglou, E. 2011, MNRAS, 414, 500, doi: 10.1111/j.1365-2966.2011.18413.x

Hewett, P. C., & Wild, V. 2010, MNRAS, 405, 2302, doi: 10.1111/j.1365-2966.2010.16648.x

Hewitt, A., & Burbidge, G. 1989, ApJS, 69, 1, doi: 10.1086/191307

HI4PI Collaboration, Ben Bekhti, N., Flöer, L., et al. 2016, A&A, 594, A116, doi: 10.1051/0004-6361/201629178

Hinton, S. R., Davis, T. M., Lidman, C., Glazebrook, K., & Lewis, G. F. 2016, Astronomy and Computing, 15, 61, doi: 10.1016/j.ascom.2016.03.001

Huo, Z.-Y., Liu, X.-W., Xiang, M.-S., et al. 2015, Research in Astronomy and Astrophysics, 15, 1438, doi: 10.1088/1674-4527/15/8/023

Ivezić, Ž., Kahn, S. M., Tyson, J. A., et al. 2019, ApJ, 873, 111, doi: 10.3847/1538-4357/ab042c

Jaunsen, A. O., Jablonski, M., Pettersen, B. R., & Stabell, R. 1995, A&A, 300, 323, doi: 10.48550/arXiv.astro-ph/9501107

Jiménez-Bailón, E., Chavushyan, V., Schartel, N., et al. 2012, AJ, 143, 64, doi: 10.1088/0004-6256/143/3/64

Jones, D. H., Read, M. A., Saunders, W., et al. 2009, MNRAS, 399, 683, doi: 10.1111/j.1365-2966.2009.15338.x

Jönsson, H., Holtzman, J. A., Allende Prieto, C., et al. 2020, AJ, 160, 120, doi: 10.3847/1538-3881/aba592

Lavaux, G., & Hudson, M. J. 2011, MNRAS, 416, 2840, doi: 10.1111/j.1365-2966.2011.19233.x

Lehner, N., & Howk, J. C. 2011, Science, 334, 955, doi: 10.1126/science.1209069

Lyke, B. W., Higley, A. N., McLane, J. N., et al. 2020, ApJS, 250, 8, doi: 10.3847/1538-4365/aba623

Majewski, S. R., Schiavon, R. P., Frinchaboy, P. M., et al. 2017, AJ, 154, 94, doi: 10.3847/1538-3881/aa784d

Mao, L. S. 2011, NewA, 16, 503, doi: 10.1016/j.newast.2011.05.002

Marchã, M. J. M., & Caccianiga, A. 2013, MNRAS, 430, 2464, doi: 10.1093/mnras/stt065

Martin, D. C., Fanson, J., Schiminovich, D., et al. 2005, ApJL, 619, L1, doi: 10.1086/426387

Masetti, N., Morelli, L., Palazzi, E., et al. 2006, A&A, 459, 21, doi: 10.1051/0004-6361:20066055

Masetti, N., Mason, E., Morelli, L., et al. 2008, A&A, 482, 113, doi: 10.1051/0004-6361:20079332

Mohammed, S., Wang, D., Schiminovich, D., & Hogg, D. W. 2019, in American Astronomical Society Meeting Abstracts, Vol. 233, American Astronomical Society Meeting Abstracts #233, 214.02

Monroe, T. R., Prochaska, J. X., Tejos, N., et al. 2016, AJ, 152, 25, doi: 10.3847/0004-6256/152/1/25

Motch, C., Belloni, T., Buckley, D., et al. 1991, A&A, 246, L24

Mullis, C. R., Henry, J. P., Gioia, I. M., et al. 2004, ApJ, 617, 192, doi: 10.1086/425248

Nagao, T., Murayama, T., & Taniguchi, Y. 2001, ApJ, 546, 744, doi: 10.1086/318300

Neeleman, M., Prochaska, J. X., Ribaudo, J., et al. 2016, ApJ, 818, 113, doi: 10.3847/0004-637X/818/2/113

O'Meara, J. M., Lehner, N., Howk, J. C., et al. 2017, AJ, 154, 114, doi: 10.3847/1538-3881/aa82b8

Pâris, I., Petitjean, P., Aubourg, É., et al. 2018, A&A, 613, A51, doi: 10.1051/0004-6361/201732445

Parisi, P., Masetti, N., Rojas, A. F., et al. 2014, A&A, 561, A67, doi: 10.1051/0004-6361/201322409

Paturel, G., Dubois, P., Petit, C., & Woelfel, F. 2002, LEDA, 0

Peeples, M., Tumlinson, J., Fox, A., et al. 2017, The Hubble Spectroscopic Legacy Archive, Instrument Science Report COS 2017-4, 8 pages

Planck Collaboration, Akrami, Y., Ashdown, M., et al. 2020, A&A, 641, A11, doi: 10.1051/0004-6361/201832618

Prochaska, J. X., Weiner, B., Chen, H. W., Mulchaey, J., & Cooksey, K. 2011, ApJ, 740, 91, doi: 10.1088/0004-637X/740/2/91

Pursimo, T., Ojha, R., Jauncey, D. L., et al. 2013, ApJ, 767, 14, doi: 10.1088/0004-637X/767/1/14

Putman, M. E., Peek, J. E. G., & Joung, M. R. 2012, ARA&A, 50, 491, doi: 10.1146/annurev-astro-081811-125612

Sabater, J., Verdes-Montenegro, L., Leon, S., Best, P., & Sulentic, J. 2012, A&A, 545, A15, doi: 10.1051/0004-6361/201118692

Schlegel, D. J., Finkbeiner, D. P., & Davis, M. 1998, ApJ, 500, 525, doi: 10.1086/305772

Shapiro, P. R., & Field, G. B. 1976, ApJ, 205, 762, doi: 10.1086/154332

Shen, Y., Brandt, W. N., Richards, G. T., et al. 2016, ApJ, 831, 7, doi: 10.3847/0004-637X/831/1/7

Snowden, S. L., Egger, R., Freyberg, M. J., et al. 1997, ApJ, 485, 125, doi: 10.1086/304399

Steinmetz, M., Zwitter, T., Siebert, A., et al. 2006, AJ, 132, 1645, doi: 10.1086/506564

Stocke, J. T., Morris, S. L., Gioia, I. M., et al. 1991, ApJS, 76, 813, doi: 10.1086/191582

Storrie-Lombardi, L. J., & Wolfe, A. M. 2000, ApJ, 543, 552, doi: 10.1086/317138

Stoughton, C., Lupton, R. H., Bernardi, M., et al. 2002, AJ, 123, 485, doi: 10.1086/324741

Su, M., Slatyer, T. R., & Finkbeiner, D. P. 2010, ApJ, 724, 1044, doi: 10.1088/0004-637X/724/2/1044

Tody, D. 1993, in Astronomical Society of the Pacific Conference Series, Vol. 52, Astronomical Data Analysis Software and Systems II, ed. R. J. Hanisch, R. J. V. Brissenden, & J. Barnes, 173

Truebenbach, A. E., & Darling, J. 2017, ApJS, 233, 3, doi: 10.3847/1538-4365/aa9026

Tumlinson, J., Thom, C., Werk, J. K., et al. 2011, Science, 334, 948, doi: 10.1126/science.1209840

Valdes, F. 1992, in Astronomical Society of the Pacific Conference Series, Vol. 25, Astronomical Data Analysis Software and Systems I, ed. D. M. Worrall, C. Biemesderfer, & J. Barnes, 417

Wegner, G., & Boley, F. I. 1993, AJ, 105, 660, doi: 10.1086/116464

Wegner, G., & Swanson, S. R. 1990, AJ, 100, 1274, doi: 10.1086/115596

Wei, J. Y., Xu, D. W., Dong, X. Y., & Hu, J. Y. 1999, A&AS, 139, 575, doi: 10.1051/aas:1999514

Wenger, M., Ochsenbein, F., Egret, D., et al. 2000, A&AS, 143, 9, doi: 10.1051/aas:2000332

Werk, J. K., Prochaska, J. X., Tumlinson, J., et al. 2014, ApJ, 792, 8, doi: 10.1088/0004-637X/792/1/8

Werk, J. K., Rubin, K. H. R., Bish, H. V., et al. 2019, ApJ, 887, 89, doi: 10.3847/1538-4357/ab54cf

Westmeier, T. 2018, MNRAS, 474, 289, doi: 10.1093/mnras/stx2757

Wilde, M. C., Werk, J. K., Burchett, J. N., et al. 2021, ApJ, 912, 9, doi: 10.3847/1538-4357/abea14

Wilde, M. C., Tchernyshyov, K., Werk, J. K., et al. 2023, ApJ, 948, 114, doi: 10.3847/1538-4357/acc85b

Wilson, R. E. 1953, Carnegie Institute Washington D.C. Publication, 0

Wright, E. L., Eisenhardt, P. R. M., Mainzer, A. K., et al. 2010, AJ, 140, 1868, doi: 10.1088/0004-6256/140/6/1868

Zheng, Y., Peek, J. E. G., Putman, M. E., & Werk, J. K. 2019, ApJ, 871, 35, doi: 10.3847/1538-4357/aaf6eb

Zheng, Y., Putman, M. E., Peek, J. E. G., & Joung, M. R. 2015, ArXiv e-prints. https://arxiv.org/abs/1504.05594